uc3m | Universidad Carlos III de Madrid

Bachelor in Aerospace Engineering
2017/2018

Bachelor's Thesis

ANALYSIS OF THE TRAJECTORY OF A HIGH-ALTITUDE BALLOON

Yolanda Marín Sabater

Supervisor:
Javier Rodríguez Rodríguez

September 2018

Abstract

The number of applications using high-altitude balloons has increased significantly in recent years. Not only because of the lower cost they represent with respect to a space mission, but also because of the advantages in terms of learning and correcting errors that they allow after their recovery. However, quantifying risks associated with it need to be considered in order to ensure the safety of those involved in the launch, as well as any person that can be affected by it. Therefore, it is needed to predict the trajectory that the balloon will follow as it is one of the main safety factors.

In this study, all the relevant physical properties of a rubber balloon will be carefully modeled and implemented in a MATLAB code, extracting the wind data from the NOAA source to create an accurate trajectory simulation program.

First, a study of the ISA atmospheric model will be performed, followed by the study of the main parameters that influence the inflation of a rubber-like balloon such as the Archimedes's Principle or the elastic effects of the rubber material.

Afterward, the kinetic equations of motion will be resolved to take into account that the horizontal motion is governing by the vagrancies of the wind, whereas the vertical motion is limited by the elastic limit of the rubber.

Finally, a validation of the software will be performed by comparing its predicted trajectory with the one obtained by two of the most well-known landing predictors, that are HABHUB and ASTRA.

Keywords: High-altitude balloon, simulator, trajectory.

Acknowledgments

This project is undoubtedly one of the most outstanding academic achievements in my short life as a university student, but I also know that it will be the beginning of a new stage in my life, full of new goals and adventures as an Aerospace Engineer. That is why I would like to thank with all my heart and dedicate my thesis to all those people who in one way or another have made me who I am, and have helped me get where I am today.

I owe my deepest gratitude to my supervisors Javier Rodríguez Rodríguez and Carolina Marugán Cruz for giving me the support, enthusiasm and motivation to make this project an unforgettable experience. I also want to express my warmest gratitude to my friends and project partners Alba, Flavia and Cristina for being a fundamental pillar in the successful development of this project.

Moreover, I would like to thanks my best friends, Sandra and Vasile, for giving me the strength to pursue my dreams and become an Aerospace Engineer; and to my aerospace fellows, especially Alba and Jose, and my mechanical engineering colleagues for all the unforgettable memories with them at university during these four years.

Heartfelt thanks go to Manuel, for being my life-buddy in all the aspects of my life and unconditionally trusting and supporting me, always making me smile through his encouragement and positivism.

Last but not least I would like to give a very special thankfulness to my family and friends, but especially to my parents, Yolanda and Ángel, and Esaú, who have been there day by day being a role model. Since childhood, they have shown me that with effort and dedication everything can be achieved. Encouraging me to work hard and keep moving forward towards my dreams. Without their support and trust in me, this would not have been possible. Thank you.

Contents

List of Figures

List of tables

1 Introduction

High-altitude balloons are an economical alternative for scientific purposes. Some of them are, space missions to test out some instruments, weather forecasting by recollecting data during the flight or conducting observations in astronomy that require a rapid response such as transients or comets, or that can not be observed from the ground [1].

However, several questions regarding high-altitude balloons, such as how far can a balloon fly? , how long does it stay in the air? or can the trajectory of a balloon be predicted, and if so, how? , still have not been resolved precisely.

Figure 1: Stratospheric balloons recollecting data in the atmosphere

Therefore, these questions will systematically be answered in the following study in order to provide a comprehensive overview of how does the balloon behaves during the flight. Nevertheless, before getting into details, a brief historical outline will be exposed in order to have a clear understanding of the evolution of the high-altitude balloons beforehand.

1.1 Background

Since the beginning of time, humanity has always admired the sky as an unknown place reserved for birds and Gods. Humans had always tried to defy the law of nature, trying to reach the sky. Archimedes, one of the best ancient Greek engineers, tried to explain the physics of a balloon flight nearly 2,000 years before the first balloon flight took place [2].

In 1783, a milestone year for aviation, the dream of flying had finally come true. On September 19th, the first hot-balloon designed by the Montgolfier brothers, Joseph and Etienne, landed in Paris after been flying for 15 minutes with 3 passengers on board: a sheep, a duck and a rooster [3].

However, the first successfully manned registered flight took place on November 21st (see **Figure 2a**), when the French scientist Pilatre de Rozier and the Marquis d'Arlandes launched from Paris and flew for a period of 20 minutes, reaching an altitude of 910 meters about the ground and covering a distance of about 9 km [3].

(a) The *Aerostat Reveillon* balloon designed by the Pilatre de Rozier (first manned flight) [4]

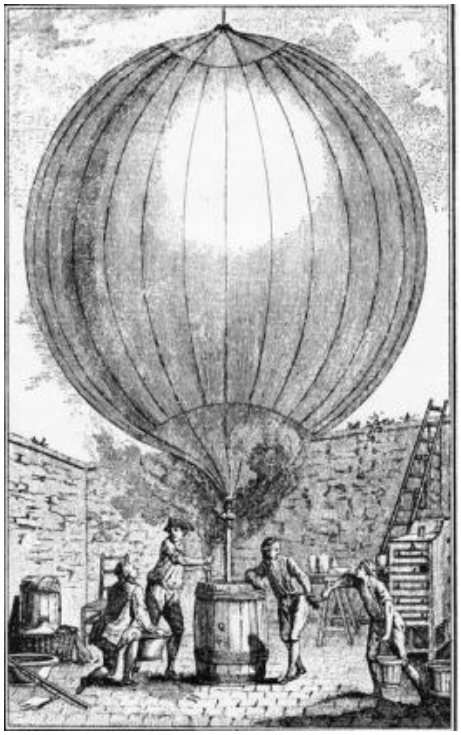

(b) First unmanned Gas-filled Balloon flight designed by Jacques Charles and the Robert brothers [5]

Figure 2: The evolution of high-altitude balloons

Nevertheless, on December 1st, Jacques Charles and the Robert brothers, Nicolas and Louis, piloted the first gas-filled balloon (see **Figure 2b**), where the envelope was filled with hydrogen instead of hot air [6].

In the following decades, several events regarding the development of balloons took place such as the first flight across the English Channel (1785), the use of balloons in the U.S. Civil War (1794-1945) or the first manned flight to the stratosphere, and first use of pressurized capsule (1932).

Subsequently, most of the effort in the development of balloon technology has focused on the evolution of the gas ballooning into high-altitude ballooning. Over the last half-century, hundreds of balloons flights have provided the science world with breathtaking images of our planet as well as invaluable data. In fact, as high-altitude balloons are a reliable, durable and dependable way of exploring the edge of the space, they were used in the development of human spaceflight [6].

1.2 Motivation

High-altitude Balloons (HAB), also known as stratospheric balloons, are aerostatic platforms filled with gas (normally hydrogen or helium) that rises among the stratosphere; in the case of this project reaching an altitude of around 30 km about the sea level [7].

Based on the ascent rate as well as the Archimedes' principle, these balloons are able to transport heavy payloads, but in this project, the payload risen will be only of around 2 kg. As it can be observed in **Figure 3**, the structure that contents and protects the payload is known as gondola which can be a pressurized volume.

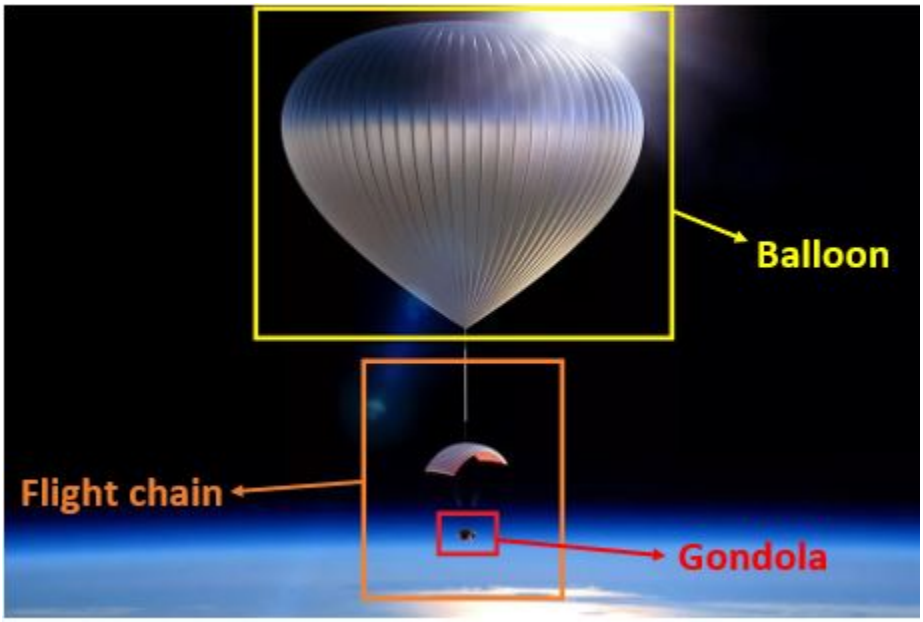

Figure 3: Main systems of a high-altitude balloon [8]

This scientific device allows the performance of stable and long-term flights, where the platform can be divided into two main systems: the balloon and the flight chain, where all the necessary subsystems for its operation such as the parachute system or the communication equipment are located [7].

As mentioned before, the use of high-altitude balloons is world-wise known. This is due to the fact that these balloons are an economical alternative to perform missions in the stratosphere as well as in the near-space region. Therefore, many entrepreneurs have seen in this type of technology a source of investment toward a new business.

However, the safety compliance issues for operational studies of the atmosphere with balloons require quantifying risks associated with it; and therefore, several strategies to reduce the uncertainties at the location of the touchdown point have been developed [9].

Hence, this study will focus on the development of a trajectory predictor that extracting the wind data from the NOAA source will give an accurate prediction of the path that the balloon will follow, as for example can be observed in **Figure 4**.

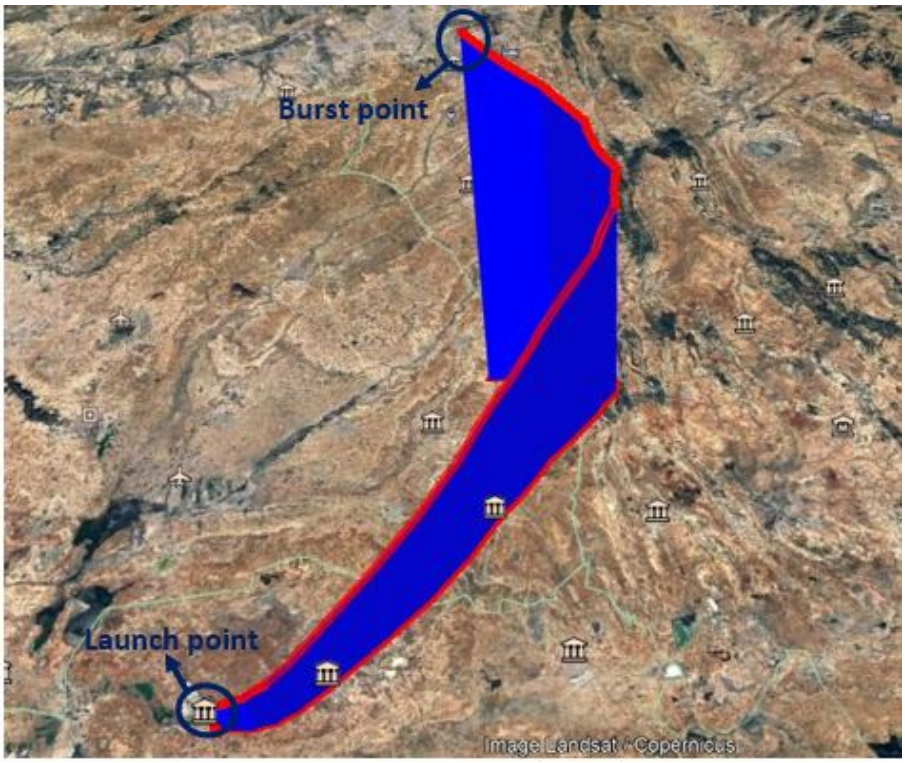

Figure 4: Predicted trajectory plotted in Google Earth

1.3 State of the art

In the last decades, several types of balloons have been used to provide mind-bending images of our planet as well as invaluable data from the stratosphere. Balloons can be divided into two main categories that are [7]:

- **Open balloons** (see **Figure 5a**), also known as **zero pressure balloons** due to the fact that the lower part is opened in order to allow the gas to expand and achieve equilibrium between the inner and the outer surface of the balloon when the altitude increases and the pressure decreases. Mainly this type of balloon is used when long-lasting flights and high payloads are desired.

- **Closed balloons** (see **Figure 5b**), also known as **super-pressure balloons** because this type of balloon is totally closed and does not allow gas flow. Therefore, as the inner pressure increases, the balloon surface expands until it achieves equilibrium. Closed balloons take about 2-3 hours to ascend, reaching a burst altitude of approximately 30 kilometers above sea level. In this study, this type of balloon will be chosen.

(a) Zero Pressure Balloon [10]

(b) Superpressure Balloon [11]

Figure 5: Types of high-altitude balloons

For several reasons, the ability to predict the trajectory of the balloon is one of the primary concerns regarding safety. The launch of high-altitude balloons is only viable if it can be performed without endangering anyone (for more details about it see **Section 4.1**) [9].

Making the forecast of the trajectory of a stratospheric balloon requires two main components that are [9]:

1. A numerical weather predictor (NWP) model, used to predict the evolution of the environmental conditions such as the wind, the radiation or the temperature.
2. A flight physics model to describe the balloon's behavior and displacements within the given environment.

Therefore, the most well-known online public landing predictors will be analyzed in order to have a global overview of how these technological tools work.

HABHUB

HABHUB is an online software formed by several tools such as a balloon burst altitude calculator, a landing predictor, and a balloon tracker; among other tools that will allow the user to obtain an accurate prediction of the trajectory that the balloon will follow. Hosted by the UKHAS (UK High Altitude Society), this landing predictor was founded by CUSF (Cambridge University Space Flight).

Moreover, analyzing the main components exposed previously about the forecasting of the trajectory of the balloon, it can be stated that:

- In this predictor, the wind data is obtained from the National Oceanic and Atmospheric Administration (NOAA) (see **Section 2.3.1** for more details). Hence, the wind data from the Global Forecasting System (GFS) is modeled in order to obtain a prediction of the path that the balloon will follow.
- The data needed to run the simulator are (see **Figure 6a**): the coordinates of the launch site, the day and time scheduled for the launch, the constant ascent and descent rates (assuming 5m/s in the case of high-altitude balloons), as well as the burst altitude. However, this last input can be calculated using the burst calculator available in HABHUB.

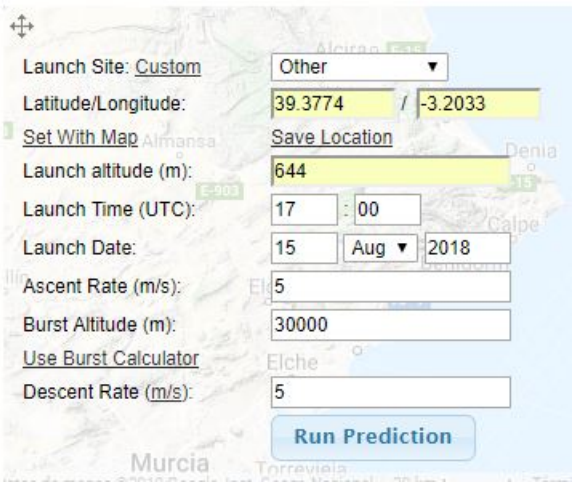

(a) Inputs needed to run the simulation

(b) Trajectory prediction

Figure 6: CUFS Landing Predictor from HABHUB [12]

The main advantages and disadvantages of this simulator are:

Advantages

✓ It is easy to use.

✓ Not many data is needed.

✓ The trajectory given is accurate enough.

Disadvantages

✗ It does not consider any thermal effects.

✗ It assumes a constant ascent and descent rate.

✗ It does not allow to simulate trajectories from the past.

ASTRA High Altitude Balloon Flight Planner

ASTRA (Atmospheric Science Through Robotic Aircraft) is a web-based predictor coded by Niccolò Zapponi. It was founded by the University of Southampton and it employs Monte Carlo techniques to randomly change the parameters of the flight, including the canopy burst diameter as well as the wind speed in order to predict the landing location [13].

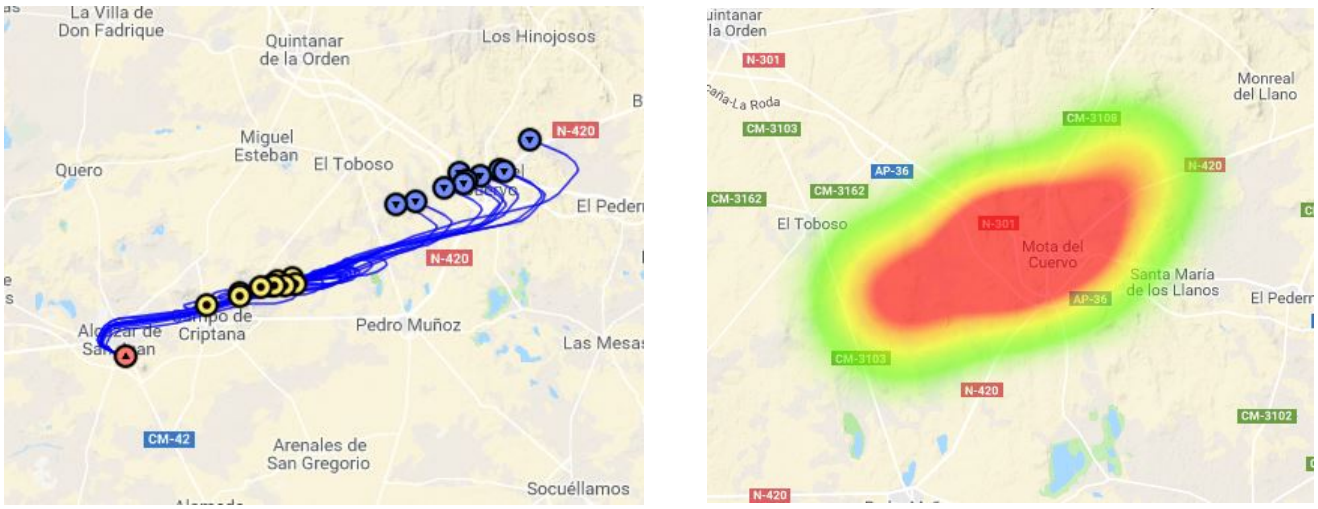

(a) Trajectory prediction (b) Landing site heat-map

Figure 7: ASTRA High Altitude Balloon Flight Planner [14]

In this predictor, the wind data is obtained using Monte Carlo techniques. Therefore, more than just the trajectory prediction can be obtained, as in the case of the landing site heat-map (see **Figure 7b**).

The main advantages and disadvantages of this simulator are:

Advantages

- ✓ It has excellent visualization features.
- ✓ It provides a landing site heat-map.
- ✓ The trajectory given is more accurate than HABHUB as it computes multiple trajectories.

Disadvantages

- ✗ More data is needed compare with HABHUB.
- ✗ It takes longer than CUSF landing predictor to run.
- ✗ It does not allow the user to enter a custom parachute or balloon canopy size.

1.4 Scope of the project

This project is based on the launch of a high-altitude balloon from "Alcázar de San Juan" (see **Section 3** for more details about why the selected location) and its collection after landing. The balloon will carry out several experiments inside the pressurized box as well as a camera to record the views of the Earth all the way from the ground to the stratosphere. Due to the magnitude of the whole project, four main groups where form with people from different backgrounds and each of the main tasks where divided. The groups are:

- The aerodynamic group, responsible for choosing the appropriate type of balloon and predict its trajectory. This study belongs to this group.
- The electronics group, in charge of choosing and programming all the electronic components such as the camera, the radio or the GPS.
- The security group, responsible for requesting all the necessary permits from EASA as well as choosing the appropriate parachute.
- The experiments group, in charge of designing and implementing the experiments in the pressurized box.

GOALS OF THIS STUDY

As it was mentioned before, the aim of this study is based on the design and implementation of an accurate software able to predict the flight path (trajectory) of the high-altitude balloon. In order to accomplished successfully this goal, the following tasks were performed:

- ✓ Selection of the type of balloon and its characteristics.
- ✓ Development of the elastic models
- ✓ Wind data research
- ✓ Design and implementation of the MATLAB's code
- ✓ Comparison with other simulators
- ✓ Verification and validation of the simulator
- ✓ Analysis of the results

Furthermore, the time needed for the development of each of the activities can be observed in **Section 4.4**.

It is important to point out, that the launch of the stratospheric balloon will take place in the weeks following to the publication of this thesis. That is why, in this study, the final validation of the simulator will not be included, since the data obtained during the flight are necessary to compare them with the data predicted by the simulator. Nevertheless, due to the fact that many people belong to this extraordinary project, the final analysis needed to certify the simulator will be presented in a future study.

2 Methodology

2.1 Atmospheric model

The first atmospheric models were developed in the 1920's in both Europe and the United States. Due to the slight differences between them, in 1952 the *International Civil Aviation Organization* (ICAO) decided to reconcile both models in an internationally accepted model known as *International Standard Atmosphere* (ISA). This model is defined in ICAO Document 7488/2 [15].

2.1.1 International Standard Atmosphere (ISA)

The International Standard Atmosphere (ISA) is a theoretical atmospheric model of how the temperature, pressure, density, and viscosity of the Earth's atmosphere change over a wide range of altitudes. This model assumes the Mean Sea Level (MSL) conditions as given:

- Pressure $\rightarrow p_0 = 101325 \ \frac{N}{m^2} = 1013.25 \ hPa$
- Density $\rightarrow \rho_0 = 1.225 \ \frac{kg}{m^3}$
- Temperature $\rightarrow T_0 = 288.15 \ K = 15°C$
- Speed of sound $\rightarrow a_0 = 340.294 \ \frac{m}{s}$
- Density $\rightarrow g_0 = 9.80665 \ \frac{m}{s}$

The different definitions of altitude known are [16]:

- Height $\rightarrow$ Vertical geometric distance between one point and the ground.
- Altitude $(z) \rightarrow$ Vertical geometric distance between one point and certain reference level (usually sea level).
- Geopotential altitude $(h) \rightarrow$ "False" altitude that would give the same potential energy in a simplified gravity field:
  - The altitude (z), is associated with the gravity acceleration that depends on it and on the latitude $(g = f(z, \psi))$.
  - The geopotential altitude (h) is associated with the sea level gravity constant (g_0).

  Therefore, the geopotential altitude and the altitude can be expressed as followed:

$$dh = \frac{g}{g_0} dz \ \ where \ \ g = f(z, \psi) \approx \frac{g_0}{(1 + \frac{z}{Re})^2}$$ being Re the radius of the Earth

For instance, in this model a small deviation of around $0.2 - 0.4\%$ takes place between the geopotential altitude (h) and the actual altitude (z), but as it is so small, it can be despised. Thus, the Standard Atmosphere is based on geopotential altitude.

2.1.2 Atmosphere Layers

The Earth's atmosphere is comprised by a series of layers, each with its own specific traits based on a constant temperature or a constant temperature gradient. Moving upward from sea level, these layers are [15, 17–19]:

- **Troposphere**: This layer goes from ground level up to 11 km altitude. Is in this part of the atmosphere where humans live, and almost all the weather conditions (clouds, rain, snow) takes place in here. As it can be observed in **Figure 8**, the troposphere is a gradient layer where temperature decreases $6.5°C/km$ with altitude.

- **Tropopause**: Separation layer at 11 km.

- **Stratosphere**: This layer goes from 11 km to 50 km altitude. Is it here, where the infamous ozone layer is found. Ozone molecules in the stratosphere, absorb the solar ultraviolet (UV) radiation, transforming it into heat. Therefore, as it can be observed in **Figure 8**, the stratosphere gets warmer the higher you move upwards.

- **Stratopause**: Separation layer at 50 km.

- **Mesosphere**: This layer goes from 50 km to 85 km altitude. Is it here, where most meteors burn up. As is shown in **Figure 8**, in the mesosphere the temperature decreases with altitude, reaching a minimum value of about $-90°C$ near the top of this layer.

- **Mesopause**: Separation layer at 85 km.

- **Thermosphere**: This layer goes from 85 km to 950 km altitude. Is it here, where most satellites orbit the Earth and Auroras takes place. As is shown in **Figure 8**, in the thermosphere, the temperature increase with altitude, caused by the absorption of energetic ultraviolet and X-Ray radiation from the Sun.

- **Exosphere**: This layer is the upper limit of the Earth's atmosphere, going from the upper part of the thermosphere to about 10000 km. It gradually fades away into the realm of interplanetary space.

  Most high-altitude balloons fly in the troposphere as well as in the stratosphere, so this study will focus on the models of these to layers.

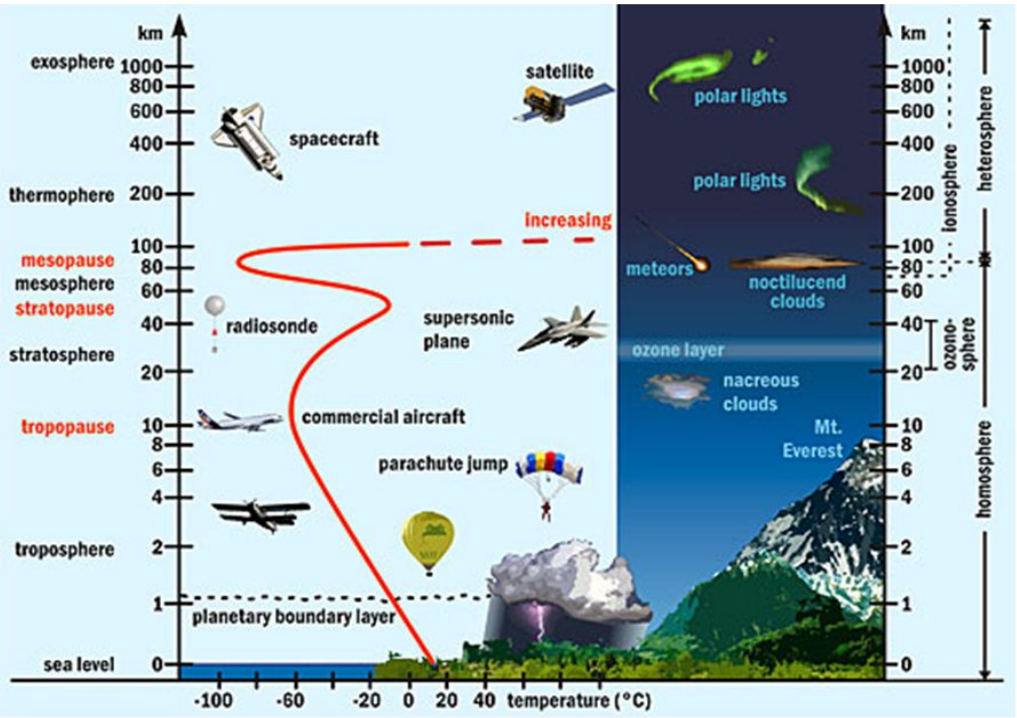

Figure 8: The Atmosphere layers and its changes in temperature due to altitude [20]

2.1.3 ISA assumptions

Under the ISO 2533:1975 environment, the following assumptions in the ISA model takes place [16]:

∗ The air is dry and a perfect gas:

$$PV = nRT \text{ where R is the gas constant with a value of } 8.3144598 \frac{J}{Kmol} \quad (1)$$

∗ The standard sea level conditions are:

Parameter	Notations	Value
Temperature	T_0	288.16 K
Pressure	P_0	101325 $\frac{N}{m^2}$
Density	ρ_0	1.225 $\frac{kg}{m^2}$

Table 1: Standard atmosphere conditions at sea level

* Acceleration due to gravity is constant at geopotential altitude, being: $g = g_0 = 9.80665 \frac{m}{s^2}$.
* Hydrostatic equilibrium yields to $dp = -\rho\, g\, dh$.
* The temperature profile in the troposphere, as mentioned before, decreased linearly with altitude up to $-56.5°C$ in the troposphere. Therefore, it is known that the gradient slope in this layer is $\alpha = 6.5 \frac{°C}{km} = 6.5 \cdot 10^{-3} \frac{K}{km}$.

2.1.4 ISA formulation

Taking into account the previous hypothesis, the following expressions are obtained for the non-dimensional variables ($\Theta, \delta \text{and} \sigma$) varying with the geopotential altitude (h), expressed in meters [16]. It is found that :

- **Troposphere** ($h \leq 11000\ m$):

$$\Theta = \frac{T}{T_0} = 1 + \frac{\alpha}{T_0} h = 1 - 2.25569 \cdot 10^{-5}\ h \tag{2}$$

$$\delta = \frac{p}{p_0} = \Theta^{\frac{-g}{\alpha \cdot R}} = \Theta^{5.2561} \tag{3}$$

$$\sigma = \frac{\rho}{\rho_0} = \Theta^{\frac{-g}{\alpha \cdot R} - 1} = \Theta^{4.2561} \ \text{ or } \ \sigma = \frac{\delta}{\Theta} \tag{4}$$

- **Tropopause** ($h = 11000\ m$):

$$\Theta_{tpp} = 0.75187 \tag{5}$$

$$\delta_{tpp} = 0.22336 \tag{6}$$

$$\sigma_{tpp} = 0.29707 \tag{7}$$

- **Stratosphere** ($h \geq 11000\ m$):

$$\Theta = \Theta_{tpp} = 0.75187 \tag{8}$$

$$\delta = \delta_{tpp} \cdot exp\left(\frac{g(h - 11000)}{R T_{tpp}}\right) = 0.22336\, exp \cdot \left(-1.57688 \cdot 10^{-4}\, (h - 11000)\right) \tag{9}$$

$$\sigma = \frac{\delta}{\Theta_{tpp}} = 1.330001\ \delta \tag{10}$$

2.1.5 ISA tables

The International Standard Atmosphere parameters (temperature, pressure, density) can be also obtained under a tabulation form, as shown in the table below [21]:

ALTITUDE (Feet)	TEMP. (°C)	PRESSURE			PRESSURE RATIO $\delta = P/Po$	DENSITY $\sigma = \rho/\rho o$	Speed of sound (kt)	ALTITUDE (meters)
		hPa	PSI	In.Hg				
40 000	- 56.5	188	2.72	5.54	0.1851	0.2462	573	12 192
39 000	- 56.5	197	2.58	5.81	0.1942	0.2583	573	11 887
38 000	- 56.5	206	2.99	6.10	0.2038	0.2710	573	11 582
37 000	- 56.5	217	3.14	6.40	0.2138	0.2844	573	11 278
36 000	- 56.3	227	3.30	6.71	0.2243	0.2981	573	10 973
35 000	- 54.3	238	3.46	7.04	0.2353	0.3099	576	10 668
34 000	- 52.4	250	3.63	7.38	0.2467	0.3220	579	10 363
33 000	- 50.4	262	3.80	7.74	0.2586	0.3345	581	10 058
32 000	- 48.4	274	3.98	8.11	0.2709	0.3473	584	9 754
31 000	- 46.4	287	4.17	8.49	0.2837	0.3605	586	9 449
30 000	- 44.4	301	4.36	8.89	0.2970	0.3741	589	9 144
29 000	- 42.5	315	4.57	9.30	0.3107	0.3881	591	8 839
28 000	- 40.5	329	4.78	9.73	0.3250	0.4025	594	8 534
27 000	- 38.5	344	4.99	10.17	0.3398	0.4173	597	8 230
26 000	- 36.5	360	5.22	10.63	0.3552	0.4325	599	7 925
25 000	- 34.5	376	5.45	11.10	0.3711	0.4481	602	7 620
24 000	- 32.5	393	5.70	11.60	0.3876	0.4642	604	7 315
23 000	- 30.6	410	5.95	12.11	0.4046	0.4806	607	7 010
22 000	- 28.6	428	6.21	12.64	0.4223	0.4976	609	6 706
21 000	- 26.6	446	6.47	13.18	0.4406	0.5150	611	6 401
20 000	- 24.6	466	6.75	13.75	0.4595	0.5328	614	6 096
19 000	- 22.6	485	7.04	14.34	0.4791	0.5511	616	5 791
18 000	- 20.7	506	7.34	14.94	0.4994	0.5699	619	5 406
17 000	- 18.7	527	7.65	15.57	0.5203	0.5892	621	5 182
16 000	- 16.7	549	7.97	16.22	0.5420	0.6090	624	4 877
15 000	- 14.7	572	8.29	16.89	0.5643	0.6292	626	4 572
14 000	- 12.7	595	8.63	17.58	0.5875	0.6500	628	4 267
13 000	- 10.8	619	8.99	18.29	0.6113	0.6713	631	3 962
12 000	- 8.8	644	9.35	19.03	0.6360	0.6932	633	3 658
11 000	- 6.8	670	9.72	19.79	0.6614	0.7156	636	3 353
10 000	- 4.8	697	10.10	20.58	0.6877	0.7385	638	3 048
9 000	- 2.8	724	10.51	21.39	0.7148	0.7620	640	2 743
8 000	- 0.8	753	10.92	22.22	0.7428	0.7860	643	2 438
7 000	+ 1.1	782	11.34	23.09	0.7716	0.8106	645	2 134
6 000	+ 3.1	812	11.78	23.98	0.8014	0.8359	647	1 829
5 000	+ 5.1	843	12.23	24.90	0.8320	0.8617	650	1 524
4 000	+ 7.1	875	12.69	25.84	0.8637	0.8881	652	1 219
3 000	+ 9.1	908	13.17	26.82	0.8962	0.9151	654	914
2 000	+ 11.0	942	13.67	27.82	0.9298	0.9428	656	610
1 000	+ 13.0	977	14.17	28.86	0.9644	0.9711	659	305
0	+ 15.0	1013	14.70	29.92	1.0000	1.0000	661	0
- 1 000	+ 17.0	1050	15.23	31.02	1.0366	1.0295	664	- 305

It is important to highlight, that 1 foot = 0.3048 meters. Therefore, the limit between the troposphere and the stratosphere takes place at 36089 ft (11000 meters).

2.1.6 ISA variations

ISA model is based on average annual conditions at latitude 45°N. Consequently, as the experiment is carried out in a different latitude, some variations should be considered in order to approach the model to the real conditions. Generally, the model is adjusted as follows [16]:

- The relation between the altitude and the pressure is maintained in this model. The pressure-altitude relation (hp) is defined as the altitude that in the standard atmosphere would produce the same pressure as measured at the aircraft.

- The variation of temperature is a shift $\Delta T(°C)$ with respect to the ISA model. For example, $ISA + 40$ represents a hotter day with respect to the standard one, while $ISA - 40$ represents a colder day compare with the standard one.

- The density is calculated with the perfect gas law (see **Equation 1**). Hence, it is important to point out that $T > 0$ (hot atmosphere) produces a lower variation of density than the standard one while $T < 0$ (cold atmosphere) produces a higher variation density as it can be observed in **Figure 9**.

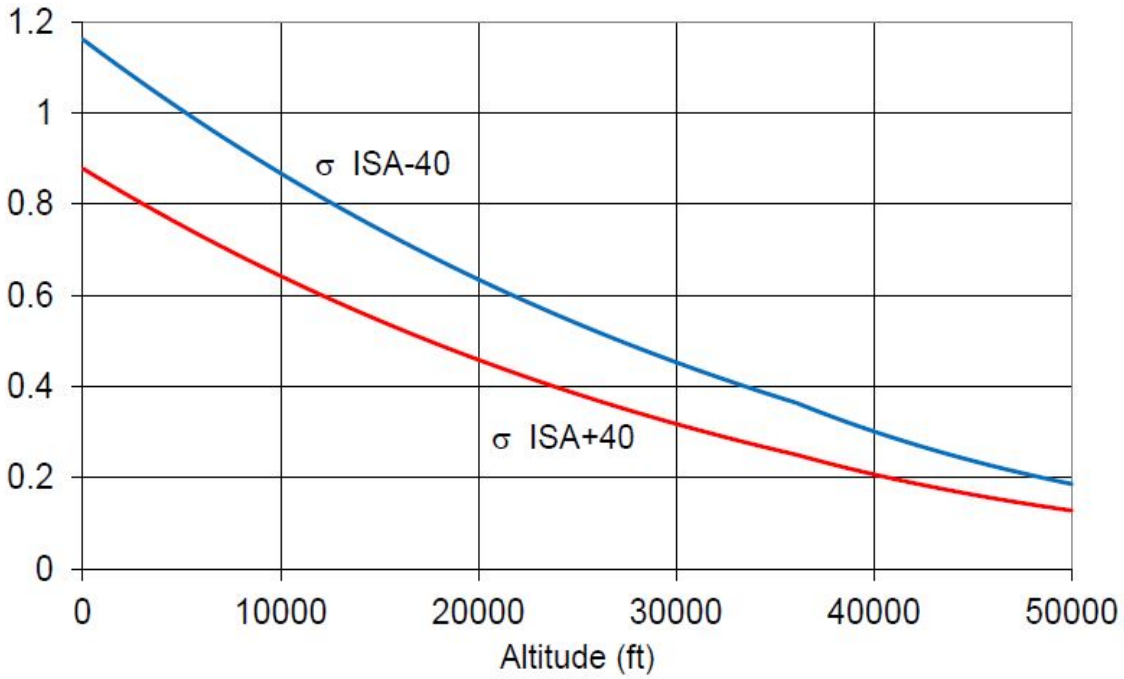

Figure 9: Variation of density ratio with ΔT [16]

2.2 The Inflation of the Balloon

2.2.1 Archimedes' Principle

Archimedes' Principle, the physical law of buoyancy, was discovered by the ancient Greek mathematician and inventor Archimedes [22]. It stated that:

Any object, wholly or partially immersed in a fluid, is buoyed up by a force equal to the weight of the fluid displaced by the object.

Therefore, this can be explained as the difference in pressure between the upper and the lower part of the surface of the object. Hence, the weight of the displaced fluid will be equivalent to the magnitude of the resulting force, known as buoyancy force. This force results in a net upward force (see **Figure 10**) produced by the difference between the greater value of pressure in the bottom part, due to the weight of the overlying fluid, and the upper part of the surface [23].

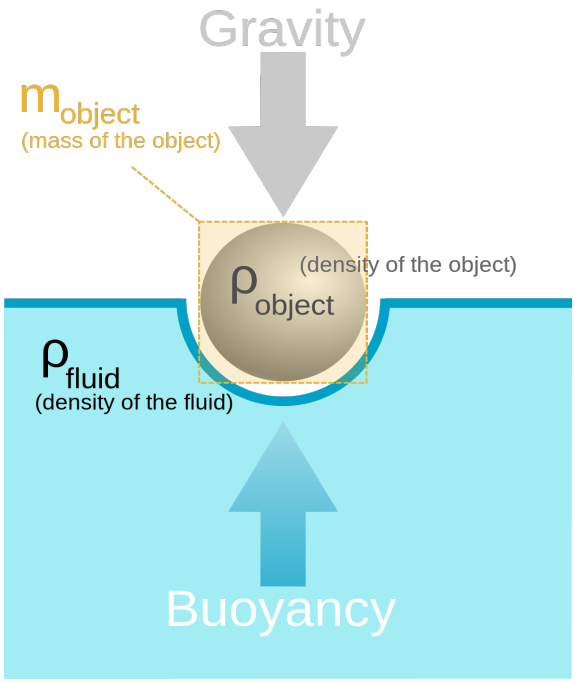

Figure 10: Buoyancy Principle [24]

If the weight of an object is less than that of the displaced fluid, the object rises, as in the case of this study, where a helium-filled balloon will be released into the air.

On the other hand, if the object is heavier than the fluid in which it is immersed, it sinks when released. Hence, the weight of the object will be equivalent to the weight of the fluid displaces [22].

Consequently, the buoyancy force (in the upward direction) can be obtained as follows:

$$F_b = p_2 S - p_1 S = \rho_{air} g (z_2 - z_1) S = \rho_{air} g V \tag{11}$$

where the variables z_1, z_2, p_1 and p_2 are represented in **Figure 11**.

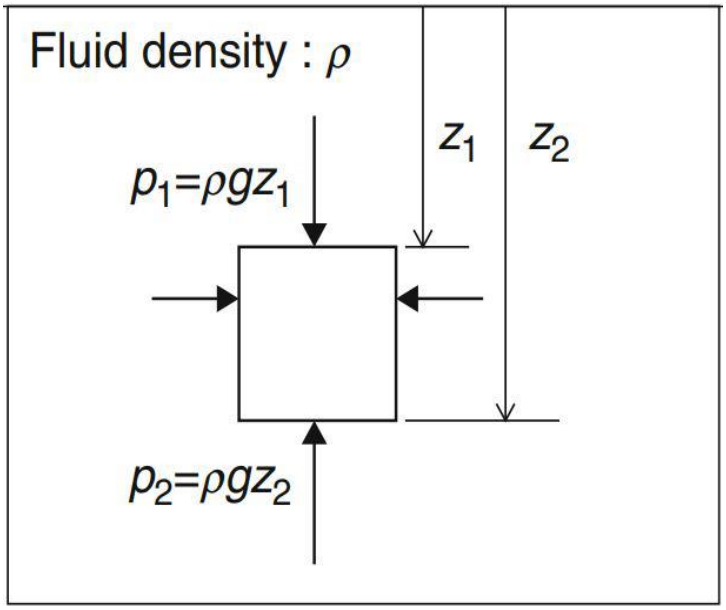

Figure 11: Reference system of the buoyancy force [25]

Furthermore, it is important to consider the difference in densities between the air (external fluid) and the helium (injected gas), so the real effective buoyancy force acting on the balloon is obtained as follows [25]:

$$\Delta F = \Delta \rho g V = (\rho_{air} - \rho_{gas}) g V \tag{12}$$

2.2.2 Balloon mass system

According to Archimedes' Principle, a balloon system in a motionless atmosphere must displace a volume of air having a weight just equal to its own weight in order to be in buoyancy equilibrium.

In practice, the most important (and most easily influenced) parameters of a balloon flight are the empty mass, the starting lift (or the balloon filling) and the choice of the fill gas. Therefore, the mass of the gross balloon can be obtained as follows [26]:

$$m_G = m_B + m_p + m_b \tag{13}$$

where

- $m_G \rightarrow$ Gross mass of the system
- $m_B \rightarrow$ Mass of the balloon
- $m_p \rightarrow$ Mass of the payload
- $m_b \rightarrow$ Mass of the ballast

Note, that the mass of the lifting gas is not included.

Therefore, the appropriate filling gas needs to be chosen. For it, the advantages and disadvantages of the hydrogen and the helium will be evaluated.

First of all, the hydrogen is lighter than the helium but a balloon filled with it will be less stable, i.e., its vertical movement is more difficult to control than that of a helium-filled balloon. Moreover, hydrogen is highly flammable in the air while helium is inert and at the same time, helium is available at a reasonable cost compared with hydrogen [26].

Thus, for this mission the gas chosen to fill the balloon was helium, and the amount of it needed will be calculated taking into consideration the characteristic of the balloon (specify in **Appendix A**) and the altitude of the launch location, using the formula below:

$$m_{He} = \rho_{air}(h_0) \cdot V_{balloon_0} \tag{14}$$

This parameter is one of the most important data to successfully fulfill the mission. However, it is known that **Equation 14** will only give the amount of helium needed to ensure the Buoyancy force (F_b), but not the real amount of helium that enters on the balloon. This can be explained due to the fact that some inaccuracies take place during the inflation process. Therefore, several studies where carried out, concluding that the amount of helium that enters the balloon only differs between 1-2 % with respect to the reference mass [27].

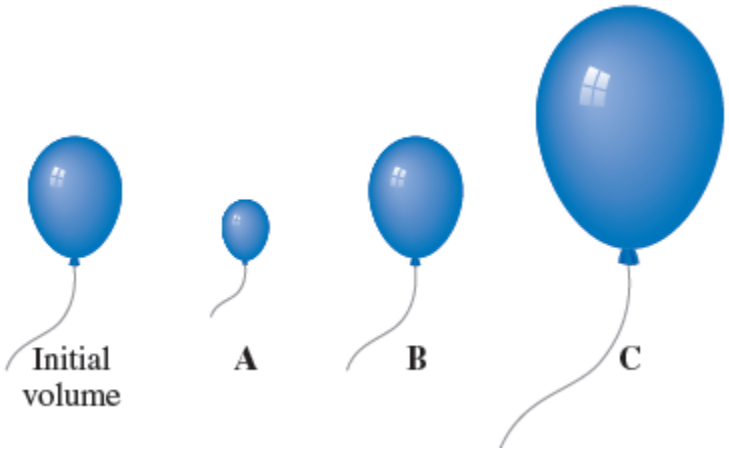

Figure 12: Possible volume cases of the balloon [28]

Moreover, as it can be observed in **Figure 12** there are three main possibilities regarding the volume of the balloon. They are:

Case A: The balloon is underfilled, what means that it will not generate the lift required to reach the desire float altitude.

Case B: The balloon is filled properly and its mission is successfully fulfilled.

Case C: The balloon is overfilled, what means that it will reach the elastic limit of the rubber before getting to the desire float altitude.

Note that only a small fraction of the balloon's volume is filled with helium on the ground. The helium expands as the balloon rises, so at float altitude, the balloon is fully inflated and nearly spherical [29].

2.2.3 Material behavior of the balloon

The material chosen for the balloons of this launch is the natural rubber latex, also known for simplicity as rubber. Rubber is a polymer, made up of a chain of mostly carbon and hydrogen. In the normal state, these chains are tangled around each other in random shapes. Different from other polymers, these chains are linked to each other through a chemical bond, known as cross-linked (see **Figure 13**). These bonds are much stronger than the intermolecular forces [30].

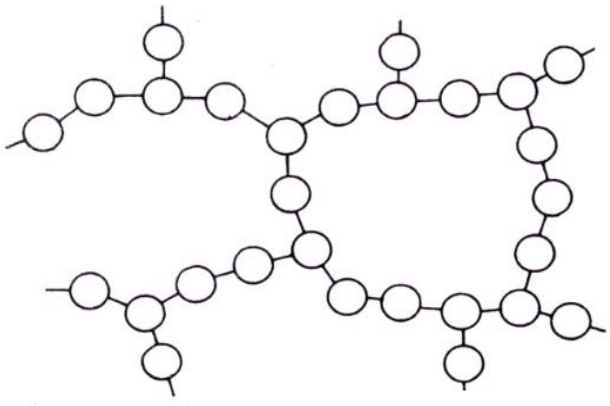

Figure 13: Cross-linked polymer [31]

Due to entropy, rubber is elastic. This means, that as a coiled up molecule is stretched out, the ways of arranging the links decreases, thus increasing the order in the system (lower entropy). When unloaded, the entropy increased again due to the fact that the system becomes more disordered as the molecules coil up, and the rubber contracts.

This leads to an unusual behavior known as the S-Shape stress-strain curve (see **Figure 14**). Therefore, as the molecules untangle and stretch out, the entropy changes and further stretching becomes easier (compare the local "elastic modulus" (slope) at the red and blue points). Afterward, as the molecules fully extended, the force starts to pull against the cross-links, and again further stretching becomes harder [30].

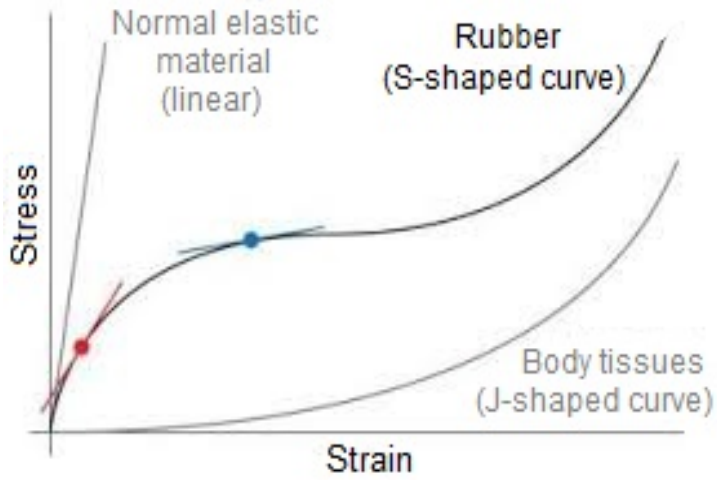

Figure 14: Stress-strain curve for rubber and some different elastic materials [30]

Aforementioned, it is known from experience that inflating a rubber balloon is difficult in the beginning, but then it becomes easier. Finally, it becomes difficult again as the balloon approaches rupture [32].

2.2.4 Elastic effects on the balloon

For an elastic balloon, the pressure inside is always a little greater than the pressure outside, due to the fact that a restoring force inwards is exerted by the rubber. In order to maximize the lift and reached the desirable float altitude, it is needed to minimize the density of the gas inside the balloon, so the extra pressure produced can be despised. However, before being able to do so, several models will be evaluated in order to understand how much effect this pressure has on the lift produced, and if it is possible to neglect it or not [33].

Hence, the effects of the inward restoring force exerted by the rubber need to be analyzed properly, considering its elasticity and comparing it with the case in which no extra pressured in taken into account.

Non-elastic model

In this model, the balloon elasticity, as well as the pressure generated by the restoring force exerted by the rubber, will be negligible. Therefore, the evolution of the radius of the balloon will be given by the ideal gas law (see **Equation 1**), obtaining that:

$$PV = nRT \Rightarrow nR = \frac{P \cdot V}{T} = \frac{P_0 \cdot V_0}{T_0} \text{ where } V_{balloon} \approx V_{sphere} = \frac{4}{3}\pi R^3 \tag{15}$$

So, the radius is expressed as:

$$R = R_0 \left(\frac{P_0}{P} \cdot \frac{T}{T_0} \right)^{\frac{1}{3}} \tag{16}$$

Moreover, the change of the thickness over time needs to be obtained. For it, the following assumptions will be considered [34]:

- The final volume should be equal to the initial volume, then as the radius increased, the thickness of the rubber will decrease.
- The terms of the order $O(t^n)$ being $n \neq 0, 1$ are very small compared to the thickness (t) and then, it can be neglected.

Applying the first assumption, it is obtained that,

$$V_F = V_0 \tag{17}$$

$$\frac{4}{3}\pi R^3 = \frac{4}{3}\pi R_0^3 \tag{18}$$

$$\frac{4}{3}\pi R_{out}^3 - \frac{4}{3}\pi R_{in}^3 = \frac{4}{3}\pi R_{out_0}^3 - \frac{4}{3}\pi R_{in_0}^3 \tag{19}$$

$$\frac{4}{3}\pi (R_{in} + t)^3 - \frac{4}{3}\pi R_{in}^3 = \frac{4}{3}\pi (R_{in_0} + t)^3 - \frac{4}{3}\pi R_{in_0}^3 \tag{20}$$

and using the second assumptions, the following equation for the thickness is found:

$$4\pi t R^2 = 4\pi t_0 R_0^2 \;\; \Rightarrow \;\; t = t_0 \left(\frac{R_0}{R} \right)^2 \tag{21}$$

Finally, as the pressure exerted by the rubber is neglected, it can be stated that the pressure difference between the inner and the outer surface of the balloon is null, and thus, $P_{in} = P_{out}$.

Gent and Mooney-Rivlin models

Nowadays, it is well-known that elastic rubber-like materials undergoing large deformations such as the inflation of a balloon (spherical thin shells), can exhibit a variety of interesting instabilities due to the appearance of a limit point instability, i.e., a point in the inflation curve where a local maximum in pressure occurs after which the volume increases with decreasing pressure. Moreover, it is known that the character of this instability depends mainly on the constitutive model used [35].

This instability led to the development of the modern non-linear elasticity models known nowadays for the inflation of balloons (thin spherical shells). In order to simplify as much as possible the calculations, the following assumptions were established [35]:

- The material used, in this case rubber, will be assumed to be hyperelastic, incompressible and isotropic.
- A purely radial deformation ($r = r(R)$) where r is the deformed radius and R is the initial radius will be assumed.
- The spherical thin shell is subjected to an internal pressure denoted as P_{in}.

Thereby, two well-known hyperelasticity models: the Mooney-Rivlin model and the Gent model will be evaluated.

1. Mooney-Rivlin model:

This model was proposed by Melvin Mooney in 1940 and expressed in terms of invariants by Ronald Rivlin in 1948.

In continuum mechanics, Mooney–Rivlin solid is a hyperelastic material model where the Strain Energy Function (SEF), "W" (see **Equation 22**), is a linear combination of the invariants of the left Cauchy–Green deformation tensor [36].

$$W = f(I_1, I_2, I_3) \tag{22}$$

Therefore, the following equation is obtained:

$$P(\lambda) = \frac{2\mu t_0}{r_0}\left(\lambda^{-1} - \lambda^{-7}\right)\left(1 + \frac{(1-\alpha)}{\alpha}\lambda^2\right) \tag{23}$$

where α is a dimensionless parameter that depends on the material of the balloon, μ is the shear modulus and $\lambda = \frac{r}{ro}$ is the principal stretch.

Mooney-Rivlin material model is one of the few famous materials models that have a very good advantage when the behavior of the hyperelastic material is unknown. In agreement with experimental observations, for a certain range of material parameters the inflation curve

have a local maximum followed by a local minimum after which the pressure increases again until the balloon bursts [35].

Therefore, the extra pressure produced by the inward force exerted by the rubber can be expressed as:

$$p_{out} = p_{in} - \Delta p = p_{in} - P(\lambda) \tag{24}$$

where introducing **Equation 23** into **Equation 24**, as well as the corresponding expressions for the external and internal pressure, gives that,

$$p_{ext}(h) - \frac{nRT(h)}{\frac{4}{3}\pi r^3} + \frac{2\mu t_0}{r_0}\left(\left(\frac{r_0}{r}\right) - \left(\frac{r_0}{r}\right)^7\right)\left(1 + \frac{(1+\alpha)}{\alpha}\left(\frac{r}{r_0}\right)^2\right) = 0 \tag{25}$$

2. Gent model:

In 1996, Alan Gent publicized a short paper that proposed the use of a simple two-parameter, shear modulus for infinitesimal deformations and a parameter that measures the maximum allowable value of strain, for hyperelastic, isotropic and incompressible materials [37].

This model is empirical but quite simple regarding mathematics. It has the advantage of modeling the stiffening that occurs as the rubber approaches breaking point; reinforced by the performance of several destructive tests in rubber balloons [33].

In 2002, an improved version of this model, known as Gent-Gent (GG), was proposed by Pucci and Saccomandi [38]. Assuming that the balloon remains spherical on inflation, the pressure difference between the atmospheric and the applied pressure can be expressed as follows [35]:

$$P(\lambda) = \frac{2\mu t_0}{r_0}(\lambda^{-1} - \lambda^{-7})\left(\frac{J_m}{J_m - (2\lambda^2 + \lambda^{-4} - 3)}\right) \tag{26}$$

where μ is the shear modulus, $\lambda = \frac{r}{ro}$ is the principal stretch and J_m is the Gent parameter.

The strain energy density function for this model is based in such a way that a singularity is obtained when the elastic limit is reached. Therefore, the Gent parameter can be considered as [37]:

$$J_m = 2\lambda_m^2 + \lambda^{-4} - 3 \tag{27}$$

Moreover, inserting **Equation 26** into **Equation 24**, as well as the corresponding expressions for the external and internal pressure, gives that,

$$p_{ext}(h) - \frac{nRT(h)}{\frac{4}{3}\pi r^3} + \frac{2\mu t_0}{r_0}\left(\left(\frac{r_0}{r}\right) - \left(\frac{r_0}{r}\right)^7\right)\frac{J_m}{J_m - \left(2\left(\frac{r}{r_0}\right)^2 + \left(\frac{r}{r_0}\right)^{-4} - 3\right)} = 0 \tag{28}$$

2.3 Wind Data Model

This model is a crucial part of the project, as the motion of the balloon will depend mainly on the accuracy of the measurement data regarding the speed of the wind. For it, a reliable source, in this case, NOAA, needs to be selected.

2.3.1 NOAA

The National Oceanic and Atmospheric Administration (NOAA) is an American research agency founded in 1970 that came up from the union of three oldest agencies that were U.S. Coast and Geodetic Survey (1807), The Weather Bureau (1870) and Commission of Fish and Fisheries (1871) [39].

This agency is dedicated to understand and predict changes in climate, weather, oceans, and coast; and to share that knowledge and information with other agencies as well as institutions, with the objective to conserve and manage coastal and marine ecosystems and resources by creating a social awareness [39].

As it can be observed in **Figure 15**, the NOAA logo illustrates the interconnection between the atmosphere, the Earth, the ecosystems and the ocean.

Figure 15: NOAA Logo [40]

About the logo design, Dr. White remarked that: *"A white, gull-like form links the atmosphere to the sea or Earth. The Earth and atmosphere and the interrelationships between the two are, of course, major concerns of NOAA. The line defining the top of the gull's wings also resemble the trough of a foaming ocean wave against the blue sky. A creature of sea, land, and air, the gull adds an ecological touch to the Earth-sky motif [40]."*

2.3.2 The NOMADS Project

The National Operational Model Archive and Distribution System (NOMADS) project is a network of data servers using established and emerging technologies to access and integrate model and other data stored in geographically distributed repositories in several different types of formats. This enables to share and compare the resulting models and serves as a source of information for several government agencies as well as academic institutions from all around the world [41].

The data measurements available under the NOMADS project are temperature, wind speed, radar data, and pressure altitude. These data can be downloaded in several formats, but the chosen one for the implementation in the MATLAB code was the ".grd2 format".

2.3.3 Trilinear interpolation

As mention in **Section 2.3.2**, the files obtained from the NOMADS project contained data from the atmosphere, beginning at the Earth's surface (sea level), all the way to the stratosphere (50 km). Therefore, the *MATLAB's NC Toolbox* (see **Appendix B** for more details) needs to be installed in order to be able to read the data required to predict the trajectory.

Inside the files, that are updated every six hours (12 a.m., 06 a.m., 12 p.m and 06 p.m.) with a validity of seven days, the variables needed for the study of the effect of the wind in the balloon and hence, in the trajectory are: *"isobaric"* that stored the pressure-altitude , *"u-component-of-wind-isobaric"* that stored the horizontal wind component and *"v-component-of-wind-isobaric"* that stored the vertical wind component.

However, even though the files contained measurement data from sea level to 50 km, only 31 values are available. Thus, a trilinear interpolation, also known as 3D interpolation, between the pressure-altitude, latitude, and longitude will be performed in order to ensure a proper prediction of the trajectory of the balloon.

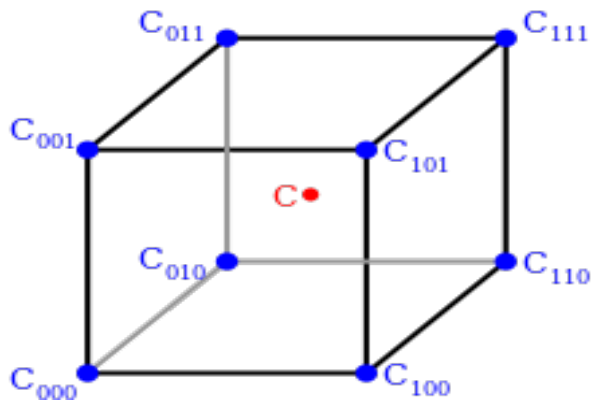

(a) Cube surrounding the interpolation point C

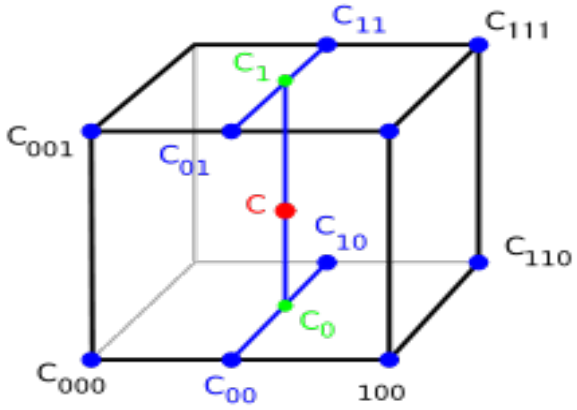

(b) The depiction of 3D interpolation

Figure 16: Trilinear interpolation

A trilinear interpolation (see **Figure 16**) is a multivariable method on a 3D dimensionless cube grid, where the value of the intermediate point is obtained by using the data from the lattice points (corners of the cube).

Furthermore, as the data obtained from the NOAA files are in an ellipsoidal coordinate system, it is necessary to transform it to Cartesian coordinates in order to be able to implement them properly in the trajectory predictor.

For it, the *MATLAB's Geodetic Toolbox* needs to be installed. This toolbox allows a direct conversion from Ellipsoidal coordinates to Cartesian coordinates.

However, this transformation needs to be considered in the equations of motion (see **Section 2.4**). Hence, the transformation coefficients from Ellipsoidal coordinates to Cartesian coordinates are expressed as:

$$R_u = \frac{\sqrt{(X_{\Delta\Phi} - X_0)^2 + (Y_{\Delta\Phi} - Y_0)^2 + (Z_{\Delta\Phi} - Z_0)^2}}{\Delta} \tag{29}$$

$$R_v = \frac{\sqrt{(X_{\Delta\lambda} - X_0)^2 + (Y_{\Delta\lambda} - Y_0)^2 + (Z_{\Delta\lambda} - Z_0)^2}}{\Delta} \tag{30}$$

where R_u stands for the longitudinal direction and R_v for the latitudinal direction. Moreover, it is important to highlight that,

$$\Delta\lambda = \lambda_0 + \Delta \tag{31}$$

$$\Delta\Phi = \Phi_0 + \Delta \tag{32}$$

represents the "real" position on the Earth's surface.

2.4 Equations of motion

As mention in the previous section (see **Sections 2.2.3** and **2.2.4**), the stratospheric balloon used in this study will be modeled as a spherical balloon for simplicity. Several studies prove that this approximation is accurate enough for the prediction of the trajectory of the balloon.

Therefore, the volume, as well as the drag coefficient used for the calculations of the trajectory, will be the ones from a sphere. Further, the elastic effects will be neglected, and the balloon will be assumed to behave as a rigid body.

During the analysis of the kinematic equations of motion, the Cartesian coordinates considered for the derivation of the equations of the trajectory of the balloon can be observed in **Figure 17**.

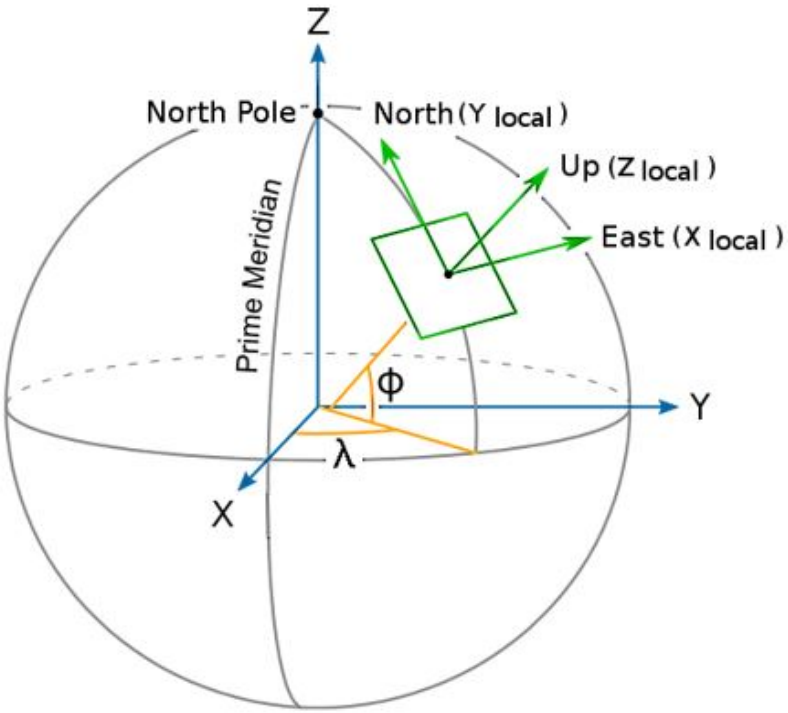

Figure 17: Cartesian to ellipsoidal coordinates in the Earth as a reference system [42]

As it can be appreciated in **Figure 17**, the x-axis corresponds to the longitudinal direction, the y-axis corresponds to the latitudinal direction and the z-axis goes from the center of the Earth towards the atmosphere.

The position of the balloon in each space of time is obtained by integrating the velocity evolution given by the Newton's Second Law (see **Equation 33**) with respect to time.

$$\Sigma \vec{F} = m \cdot \vec{a} \tag{33}$$

In z-direction, the motion of the balloon is described by the "first equation of motion" (**see Equation 34**) and the "second equation of motion" (**see Equation 35**). These equations are expressed as follows:

$$\frac{dh}{dt} = v \tag{34}$$

$$m\frac{dv}{dt} = T - W - D_v \tag{35}$$

where it is known that,

$$T = \rho(h)gV(h) \tag{36}$$

$$W = m_T g \tag{37}$$

$$D_v = \frac{1}{2}\rho(h)v^2 A(h)C_D \tag{38}$$

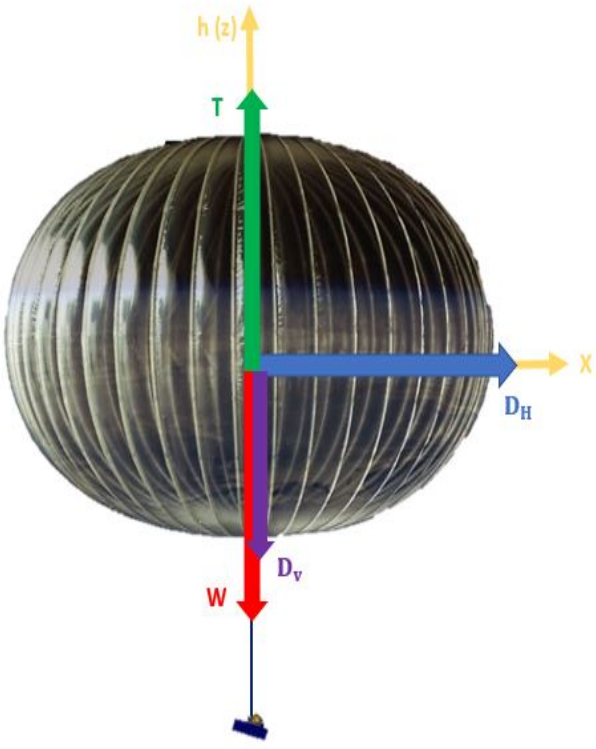

Figure 18: Reference system in the balloon and the forces applied to it

As it can be observed in (**Figure 18**), the thrust (T) moves upwards in the z-direction, while the weight (W) moves downwards in the same direction.

On the hand, it is shown that the horizontal drag (D_H) moves towards the East in the x-direction while the vertical drag (D_v) moves downwards in the z-direction.

In x-direction, the motion of the balloon is described by the "third equation of motion" (**see Equation 39**) and the "fourth equation of motion" (**see Equation 40**). These equations are expressed as follows:

$$\frac{dx}{dt} = v_x \tag{39}$$

$$\frac{W}{g} \cdot \frac{dv_x}{dt} = \frac{1}{2}\rho(v_{wind_x} - v_x)^2 A C_D \tag{40}$$

In y-direction, the motion of the balloon follows a similar evolution as it does in the x-direction. Therefore, this motion is described by the "fifth equation of motion" (**see Equation 41**) and the "sixth equation of motion" (**see Equation 42**) that are similar to the "third and fourth equation of motion", respectively. These equations are expressed as follows:

$$\frac{dy}{dt} = v_y \tag{41}$$

$$\frac{W}{g} \cdot \frac{dv_y}{dt} = \frac{1}{2}\rho(v_{wind_y} - v_y)^2 A C_D \tag{42}$$

Notice, that the Coriolis force is not considered. This can be briefly explained due to the fact that the effect produced by this force in the trajectory of short flights, such as the one studied in this project, is of the order of 10^{-4}; and hence, it will suppose a deviation of about 150 m at the end of the trajectory. Therefore, this force will be neglected, and the balloon is assumed to be a perfect plotter without any deviation.

3 Stratospheric Balloon Mission

After the MATLAB code was implemented (see **Appendix B**), the following results were obtained:

3.1 Results of the elastic effect on the balloon

As it was mentioned earlier in **Section 2.2.4**, any elastic balloon filled with helium will experience an inward restoring force exerted by the rubber. Then, the effect that this force generated in the balloon will be analyzed in detail by studying the performance of the radius, the membrane pressure, the lift, and the ascent velocity rate for each of the three models mentioned above, that are the non-elastic model, the Mooney-Rivlin model and the Gent-Gent model.

3.1.1 Radius evolution with altitude

It is important to point out, that the radius evolution in the non-elastic model will be obtained considering that the volume of the rubber balloon is constant during the ascent phase. On the other hand, in the case of the Mooney-Rivlin model and the Gent-Gent model the radius evolution with altitude will be obtained by solving **Equation 25** and **28**, respectively. The result obtained after implementing these models in the MATLAB code (see the *elasticity function* from the **Appendix B** for more details) is:

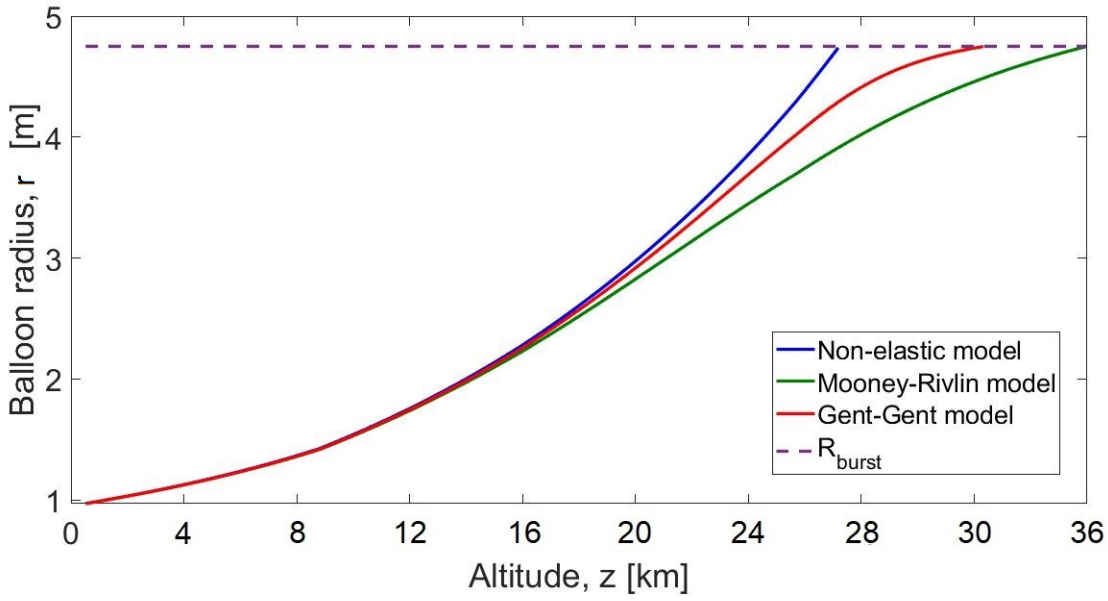

Figure 19: Radius evolution with altitude

As it can be observed in **Figure 19**, the burst diameter given by the technical specifications (see **Appendix A**) of the chosen balloon stated that it has an approximate value of 9.5 m, hence a burst radius of 4.75 m. Considering this value, it can be seen that burst altitude occurs at 27.5 km for the non-linear model, at 35.2 km for the Mooney-Rivlin model and at 33.25 km for the Gent-Gent model.

If these values are compared with the burst altitude of 34 km given by the manufacturer, it can be noticed that in the case of the non-linear model a smaller radius is obtained. This can be explained due to the fact the pressure difference increases faster as the altitude becomes higher. However, in the case of the other two models, the values are quite close compare to the given data; and it can be stated that in these cases elasticity does not have a relevant effect on the ceiling altitude.

3.1.2 Pressure difference

Afterward, a depth study of the pressure difference exerted in the membrane will be performed in order to evaluate its behavior regarding altitude.

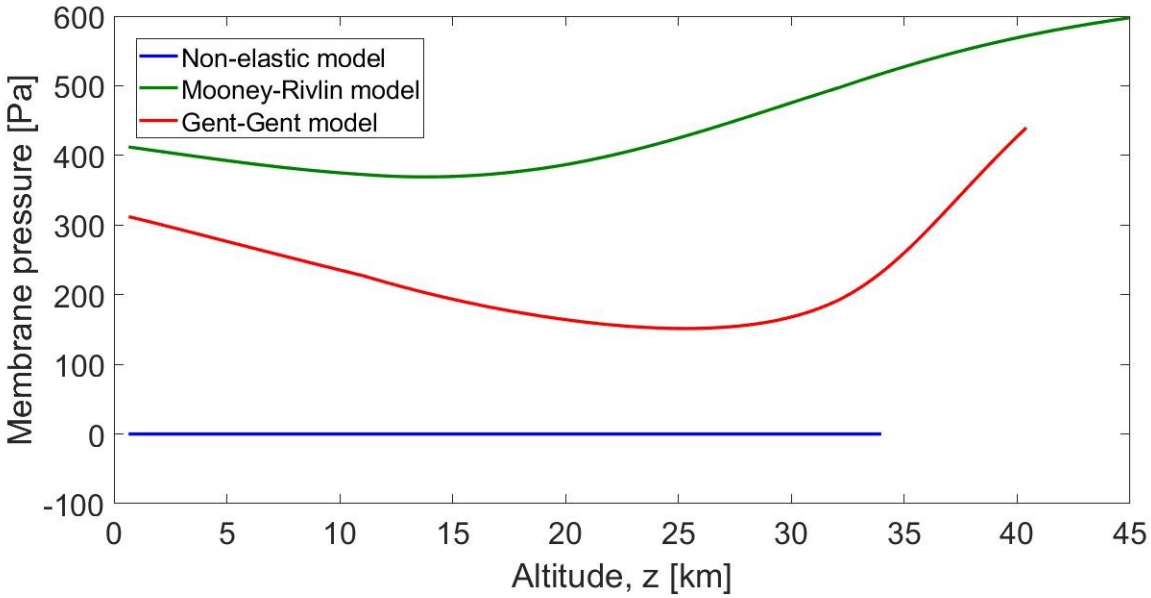

Figure 20: Membrane pressure evolution with altitude

As it is shown in **Figure 20**, the pressure difference in the case of the non-elastic model is zero as non-restoring forces are considered; whereas in the case of the Mooney-Rivlin and the Gent-Gent model a value of 305 Pa and 408 Pa, respectively, at sea level is obtained.

Moreover, it can be observed that the pressure in the flight envelope is between 175 and 500 Pa, what means that this pressure can be neglected at low altitudes, as the atmospheric pressure at launch altitude is of the order of 100, 000 Pa.

However, as pressure decreases with increasing altitude at low altitudes, a deeper study regarding this effect at high altitudes was conducted. It was proved that after 38 km the membrane pressures begins to be important and hence, it should be considered.

Taking into account that the studied balloon can only reach a maximum altitude of 34 km, it can be concluded that for the implementation of the trajectory simulator, the effect of the membrane pressure can be neglected.

3.1.3 Lifted mass

As it was explained in **Section 2.2.1** the mass of air displaced by the balloons, also known as lift mass, is equivalent to its own weight in order to ensure buoyancy equilibrium.

Therefore, the lifted mass can be computed as:

$$m_{lift} = \rho(z) \cdot V_{balloon}(z) \tag{43}$$

Analyzing **Equation 21**, it can be ensured that in the non-linear model the lifted mass will remain constant as the membrane pressure is not considered and hence, the volume of the balloon doesn't change during the ascent phase.

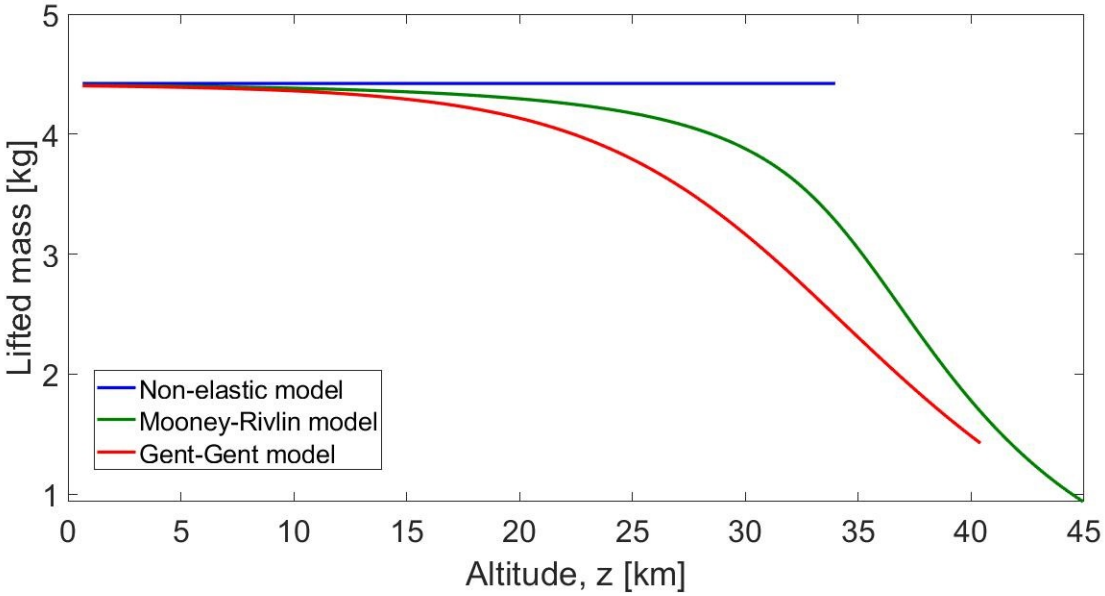

Figure 21: Lift curve

On the other hand, as it can be seen in **Figure 21** in the Mooney-Rivlin model and in the Gent-Gent model, the lifted mass decreases with increasing altitude. This can be explained because the density of the air decreases with altitude much faster than the increase in the volume of the balloon.

Under the Mooney-Rivlin model, the lifted mass decreases from 4.4 kg at launch altitude to 3.3 kg at burst altitude, whereas in the case of the Gent-Gent model the lifted mass drops from 4.4 kg at launch altitude to 2.5 kg at burst altitude. However,as it is mentioned in the specification conditions (see **Appendix A**) this decrease in the lifted mass does not have any repercussions in the performance of the ascent phase of the balloon's trajectory.

3.1.4 Ascent velocity

Furthermore, the ascent velocity in each of the three models will be evaluated considering as a simplification of the drag coefficient of a sphere ($C_{D_{sphere}} = 0.47$). As it can be notified in **Figure 22**, the ascent velocity increases with increasing altitude. This can be explained, due to the fact that the lift generated by the helium mass is greater than the drag force produced by the decrease in the air density as altitude increases.

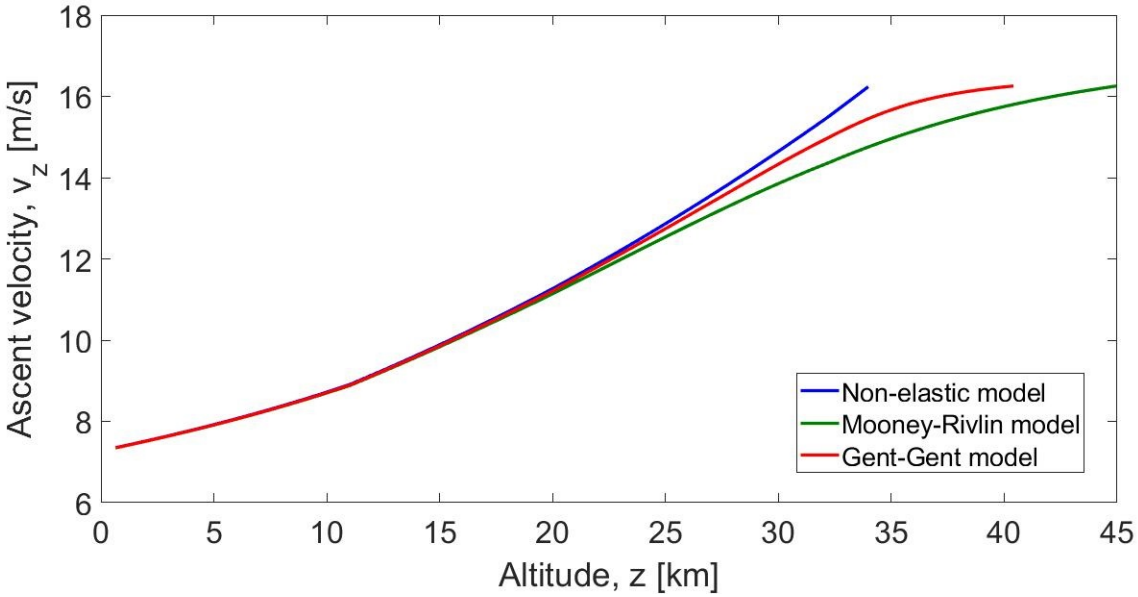

Figure 22: Ascent velocity with altitude

Therefore, the ascent velocity can be obtained by clearing it from the equalization of the vertical drag and the weight of the lifted mass, obtaining that:

$$D_v = W_{lifted} \Rightarrow \frac{1}{2}\rho v_z^2 A C_D = m_{lift} g \Rightarrow v_z = \sqrt{\frac{2 g m_{lift}}{C_D \pi \rho(z) R^2(h)}} \tag{44}$$

It can be pointed out, that the initial ascent rate is around 7.4 m/s or 444 m/min, which is larger than the ascent rate of 325 m/min specified by the manufacturer. However, if we computed the average ascent rate, a value of 323.8 m/min is obtained as the whole ascent phase takes about 105 minutes to rise up to 34 km about sea level.

3.2 Trajectory prediction of the high-altitude balloon

In this section, the results obtained by the simulation of the trajectory of the high-altitude balloon for a chosen day, in this case, the $7^{\underline{th}}$ of September of 2018, will be presented. It is important to highlight, that the developed software will only evaluate the ascent part of the trajectory.

After evaluating for several months what would be the ideal place to launch the balloon and ensuring that the trajectory prediction fulfills all the legal requirements (see **Section 4.1** for more details), the launch point selected was *"Alcázar de San Juan"*. This place is located at 644 m of altitude and its coordinates are [39.3774, -3.2033].

As it was mention in **Section 2**, the trajectory of the balloon is mainly influenced by the direction of the wind. Therefore, it is known that the horizontal motion of the balloon will be dictated solely by the vagrancies of the wind.

As it can be observed in **Figure 23a** and **Figure 23b** the horizontal motion of the balloon for this specific case around the surface of the Earth is:

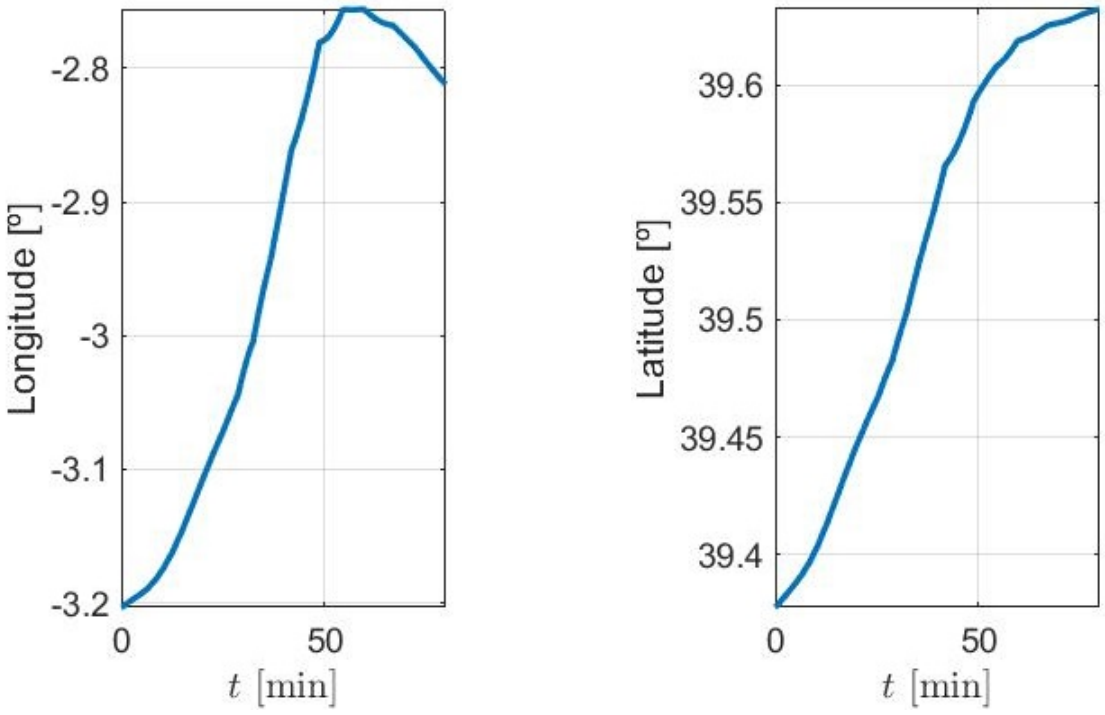

(a) Longitudinal direction (x-coordinate) (b) Latitudinal direction (y-coordinate)

Figure 23: Position of the balloon over time around the Earth's surface

Moreover, if the velocity of the horizontal motion is analyzed, it can be seen (see **Figure 24**) that an irregular profile with several peaks is obtained. This can be explained, due to the fact that a trilinear interpolation (see **Section 2.3.3**) was performed as only 31 values are available in the NOAA files.

However, although there are fluctuations in the speed of the wind, the trajectory is not affected since to obtain it, it is necessary to integrate it and therefore, it is an average.

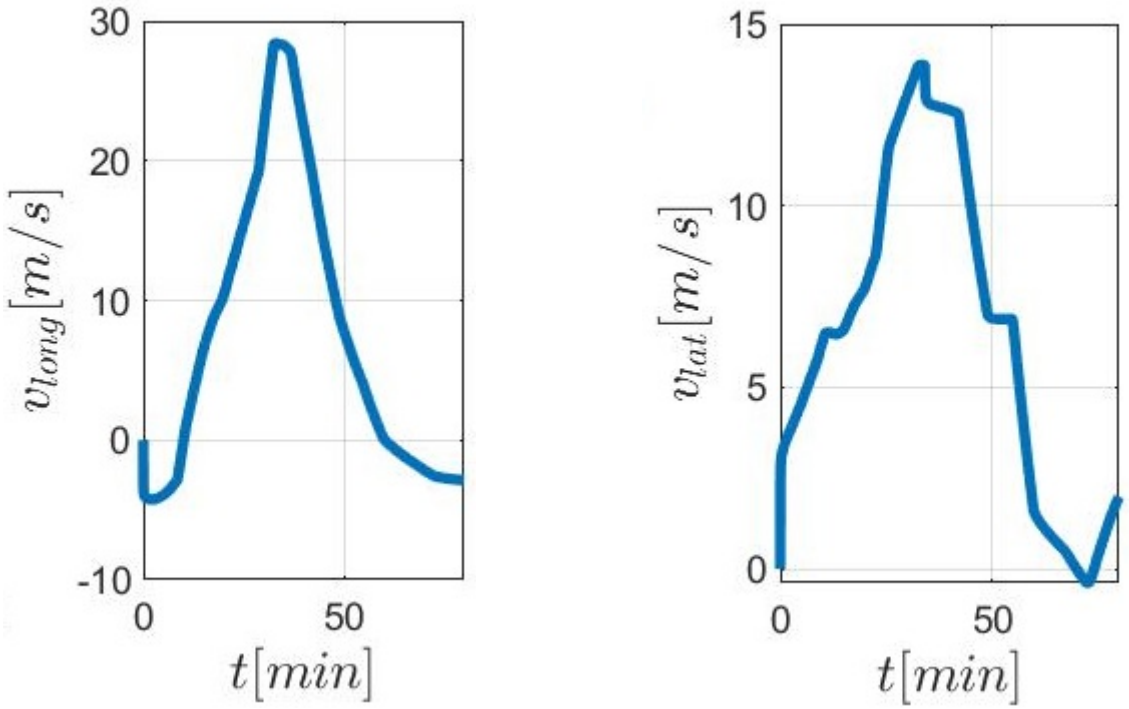

(a) Longitudinal direction (x-coordinate)

(b) Latitudinal direction (y-coordinate)

Figure 24: Velocity of the balloon over time during the ascent phase

As it can be observed in the left graph of **Figure 25**, the temporal evolution of the altitude, in the developed software, experiences an almost exponential growth. This can be explained, due to the assumption that the interior temperature of the balloon is the same as the exterior temperature, and hence, the expansion of the balloon is constant, following the ideal gas law.

Furthermore, is important to point out the independence of the altitude of the balloon with respect to the wind. This is, because the file provided by the NOAA source only contains data of the wind in 2D, without providing any information regarding the direction perpendicular to the Earth. This allows eliminating any uncertainty of the weather predictions in the vertical trajectory.

As it can be seen in the right graph of **Figure 25**, straight away after the balloon is released, the ascent velocity reached a value of about 4.75 m/s. However, this velocity keeps increasing exponentially until reaching a value of 9 m/s before exploding.

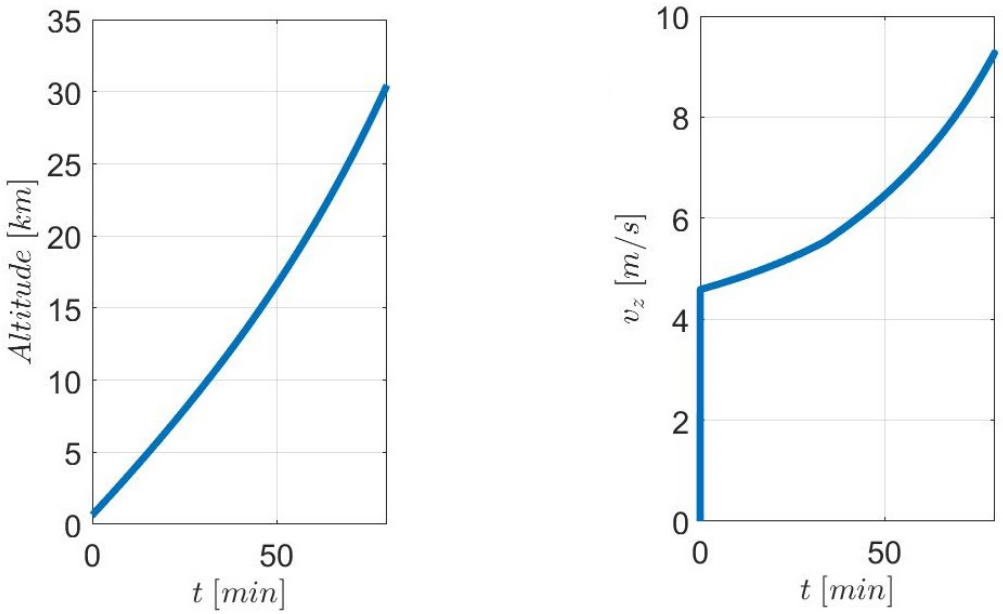

(a) Position over time

(b) Velocity over time

Figure 25: Temporal evolution in the z-direction (perpendicular to the Earth's surface)

After evaluating each of the directions with respect to time, the following trajectory taking off from *"Alcázar de San Juan (Spain)"* is obtained:

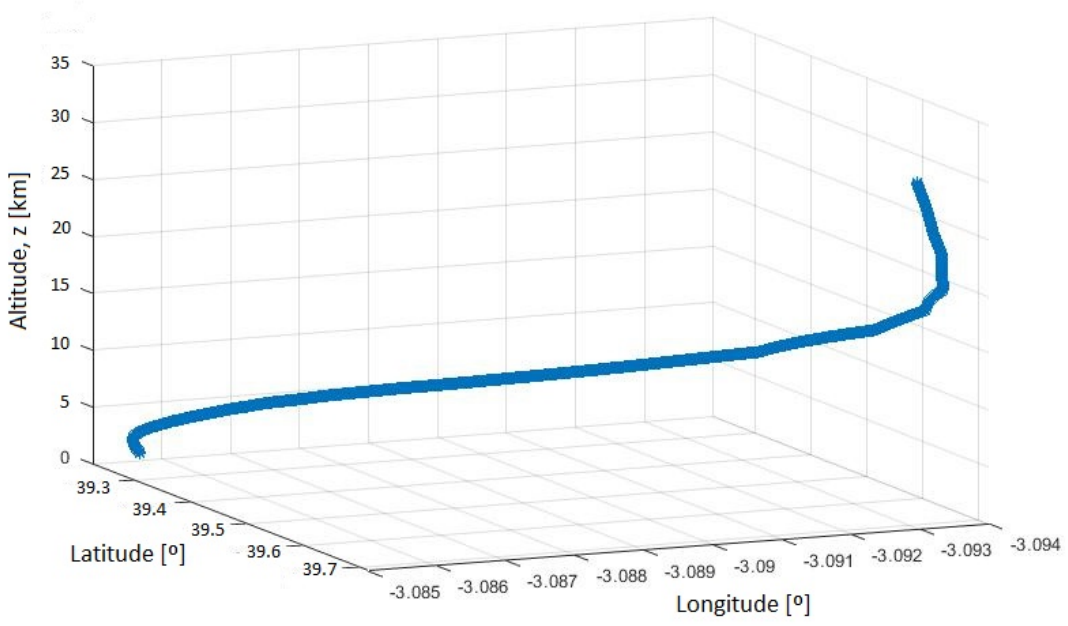

Figure 26: Trajectory prediction around the Earth's surface

3.3 Software validation

3.3.1 Comparison with other predictors

Finally, a validation of the simulator will be performed in order to ensure that the predictor works properly. For it, the flight path obtained with the developed software will be compared with two of the most well-known landing predictors, as it was explained in **Section 1.3**.

Notice that in **Figure 27**, the blue trajectory corresponds to the developed software, the yellow trajectory belongs to the CUSF Landing Predictor from HABHUB and the red trajectory is obtained from ASTRA.

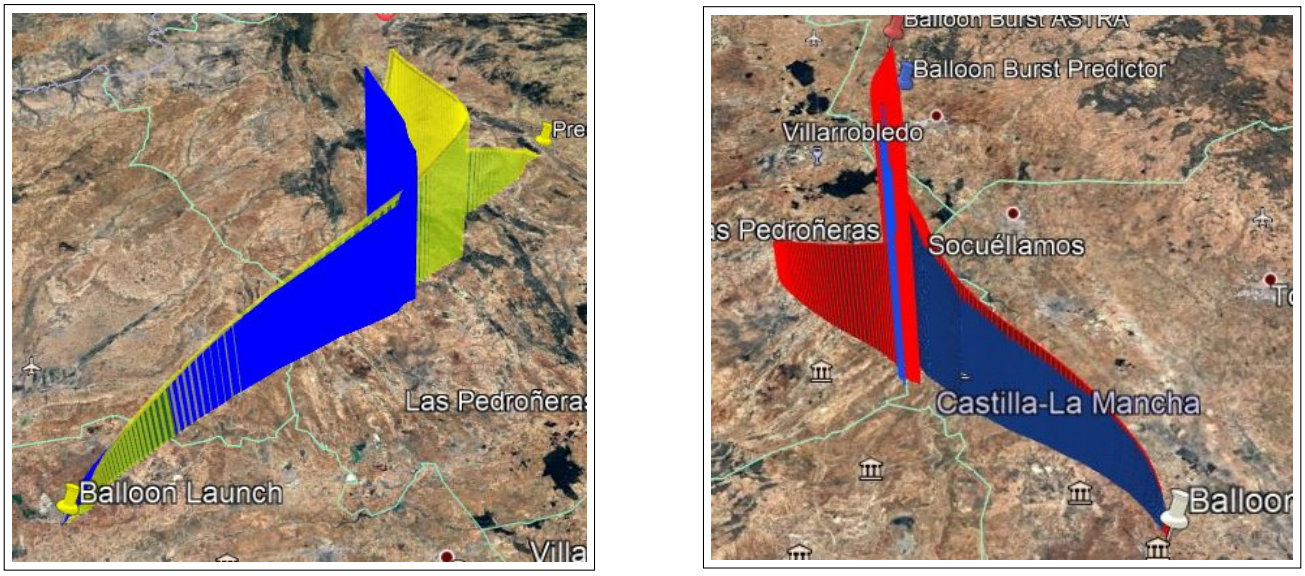

(a) HABHUB (b) ASTRA

Figure 27: Comparison of the trajectory obtained with two web-based predictors

Therefore, the trajectory obtained with each of them will be plotted using Google Earth, and the following differences were observed:

Comparison with HABHUB (CUSF Landing Predictor)

As it can be seen in **Figure 27a**, both trajectories reached almost the same burst altitude, although the obtained trajectory gets to it faster than the trajectory predicted by HABHUB. This can be addressed as a factor that the CUSF Landing Predictor takes a constant ascent rate; while in the case of the developed software, the ascent rate is obtained from the principles of physics and the resolution of the equations of motion of the balloon (see **Section 2.4** for more details).

Comparison with ASTRA (High Altitude Balloon Flight Planner)

As it can be observed in **Figure 27b**, both trajectories get to the burst altitude at the same time. However, ASTRA predicts a higher burst altitude than the one obtained with the developed software. This can be justified due to the fact that although ASTRA is a very precise software, it imposes the selection between certain predetermined types of high-altitude balloons; and the one chosen for this study and implemented in the developed-software was not included in the available options. Nevertheless, a similar balloon was chosen to run the ASTRA predictors.

3.3.2 Numerical comparison

Finally, a numerical comparison between the three predictors will be performed in order to verify that the developed software describes an accurate trajectory of the balloon. In **Figure 28**, the trajectory of the $7^{\underline{th}}$ of September of 2018 at 3 p.m of each of the three predictors can be observed, where the selected launch point is *"Alcázar de San Juan"*.

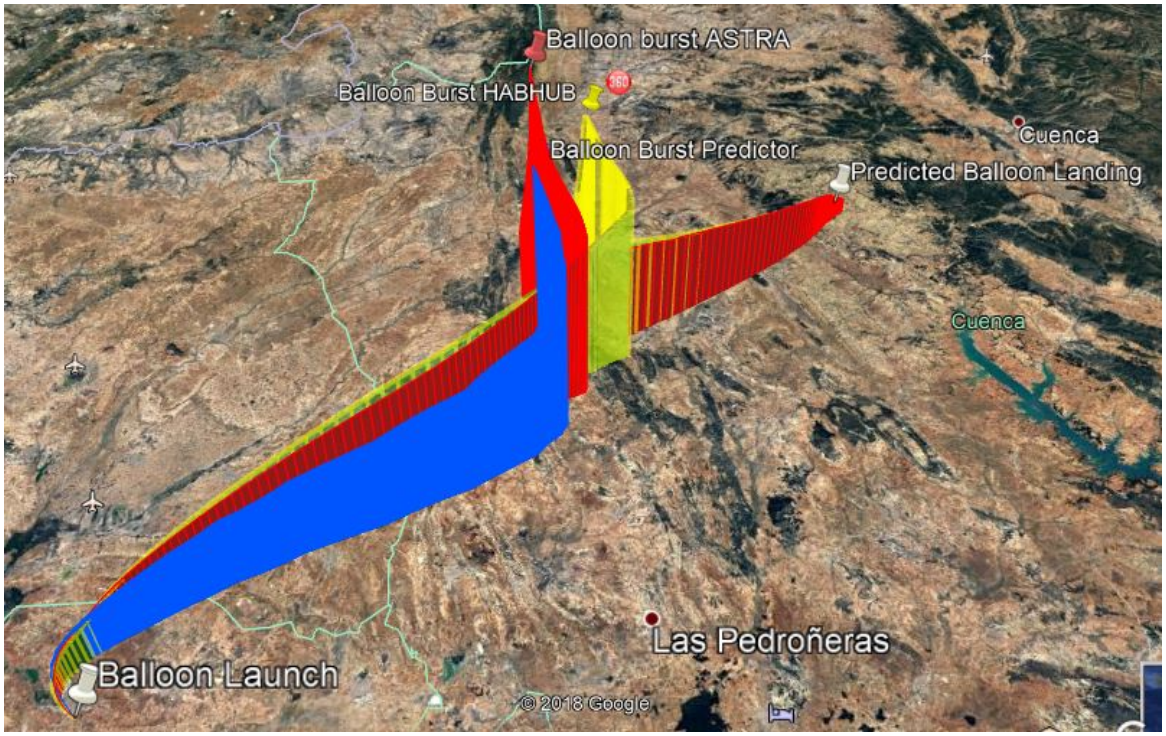

Figure 28: Comparison of the trajectory of the different predictors

As it was mentioned before, the blue trajectory corresponds to the developed software, the yellow trajectory belongs to the CUSF Landing Predictor from HABHUB and the red

trajectory is obtained from ASTRA. Therefore, the following values regarding the burst altitude were obtained:

	Burst altitude	Coordinates Burst point
Developed software	**30458 m**	**[39.6581 , -2.7853]**
HABHUB	**29694 m**	**[39.7276 , -2.7388]**
ASTRA	**36945 m**	**[39.6967 , -2.7890]**

Table 2: Predicted burst data

It can be pointed out, that the highest burst altitude is predicted by ASTRA with a value of 36945 m, exceeding by more than 6000 meters compared to the other two predictors. This can be explained mainly for two reasons.

The fist one is, as it was mentioned before ASTRA imposed the selection between certain predetermined types of balloons, and the one chosen for this study was not included. Therefore, a similar balloon was chosen; although the material of the balloon is not the same, and therefore, its elastic limit is different; allowing it to reach a higher burst altitude.

The second reason is that HABHUB and the developed software takes the wind data directly from the NOAA source, whereas ASTRA takes them from another source. Hence, there may be some slightly different values with respect to the wind speed used to predict the trajectory.

Furthermore, it can be highlighted that even though each of the predictors used a different way to approach the ascent rate trajectory (see **Sections 1.3 and 3.3** for more details), the coordinates of the point at which the burst altitude takes place are very similar, as it can be seen in **Table 2**.

Finally, it can be concluded that the developed software for the prediction of the trajectory of the ascent phase of a high-altitude balloon is pretty accurate. Nevertheless, the final validation will take place after the data from the launch is recollected; however, this final validation stage is out of the scope of this thesis.

4 Legal and Socio-economic Framework

In this section, several aspects regarding governmental as well as economic values will be exposed in order to have a clear understanding of the main issues in these fields regarding this type of technology.

4.1 Legal Framework

Over 500,000 high-altitude balloons, also known as weather balloons, are launched around the world every year. Most are for government meteorological or research purposes, but over 3,000 educational and amateur flights are also conducted every year across the globe [43]. Therefore, several governing laws and regulations are established in order to ensure the safety of those involved in the launch, as well as any person that can be affected by it.

Every country has its own regulations surrounding high-altitude balloons flights. It is critical to understand and follow them properly, in order to avoid any type of potential risk. In most cases, a permission in advance is needed and the day of the launch, the flight must be notified to the governing organization.

In the member countries of the European Union (EU), the agency in charge of the air traffic safety regulations is the European Aviation Safety Agency (EASA). This agency has issued a *Balloon Rule Book* [44] that include some certification specifications as well as acceptable means of compliance for gas balloons. However, these regulations are not related to high altitude balloons and due to this fact, the American regulations issued by the Federal Aviation Administration (FAA) and the Federal Communication Commission (FCC) will be taken as the legal framework for this study.

According to the Federal Aviation Administration and the Federal Communication Commission the following laws and regulations for "Unmanned Free High-altitude Balloons" need to be fulfill. These regulations are:

FAA (Title 14: Aeronautics and Space, Chapter I, Subchapter F, Part 101 [45])

§101.31 Applicability.

This subpart applies to the operation of unmanned free balloons. However, a person operating an unmanned free balloon within a restricted area must comply only with **§101.33 (d)** and **(e)** and with any additional limitations that are imposed by the using or controlling agency, as appropriate.

§101.33 Operating limitations.

"No person may operate an unmanned free balloon... "

(a) *"Unless otherwise authorized by ATC, below 2,000 feet above the surface within the lateral boundaries of the surface areas of Class B, Class C, Class D, or Class E airspace designated for an airport;"*

(b) *"At any altitude where there are clouds or obscuring phenomena of more than five-tenths coverage;"*

(c) *"At any altitude below 60,000 feet standard pressure altitude where the horizontal visibility is less than five miles"*

(d) *"During the first 1,000 feet of ascent, over a congested area of a city, town, or settlement or an open-air assembly of persons not associated with the operation; or"*

(e) *"In such a manner that impact of the balloon, or part thereof including its payload, with the surface creates a hazard to persons or property not associated with the operation."*

§101.35 Equipment and marking requirements.

(a) *No person may operate an unmanned free balloon unless:*

(1) *"It is equipped with at least two payload cut-down systems or devices that operate independently of each other"*

(2) *"At least two methods, systems, devices, or combinations thereof, that function independently of each other, are employed for terminating the flight of the balloon envelope; and"*

(3) *"The balloon envelope is equipped with a radar reflective device(s) or material that will present an echo to surface radar operating in the 200 MHz to 2700 MHz frequency range"*

(b) *"No person may operate an unmanned free balloon below 60,000 feet standard pressure altitude between sunset and sunrise (as corrected to the altitude of operation) unless the balloon and its attachments and payload, whether or not they become separated during the operation, are equipped with lights that are visible for at least 5 miles and have a flash frequency of at least 40, and not more than 100, cycles per minute."*

(c) *"No person may operate an unmanned free balloon that is equipped with a trailing antenna that requires an impact force of more than 50 pounds to break it at any point, unless the antenna has colored pennants or streamers that are attached at not more than 50 foot intervals and that are visible for at least one mile."*

(d) *"No person may operate between sunrise and sunset an unmanned free balloon that is equipped with a suspension device (other than a highly conspicuously colored open parachute) more than 50 feet along, unless the suspension device is colored in alternate*

bands of high conspicuous colors or has colored pennants or streamers attached which are visible for at least one mile."

§101.37 Notice requirements.

(a) *"Prelaunch notice: Except as provided in paragraph (b) of this section, no person may operate an unmanned free balloon unless, within 6 to 24 hours before beginning the operation, he gives the following information to the FAA ATC facility that is nearest to the place of intended operation:"*

(1) *"The balloon identification."*

(2) *"The estimated date and time of launching, amended as necessary to remain within plus or minus 30 minutes."*

(3) *"The location of the launching site."*

(4) *"The cruising altitude."*

(5) *"The forecast trajectory and estimated time to cruising altitude or 60,000 feet standard pressure altitude, whichever is lower."*

(6) *"The length and diameter of the balloon, length of the suspension device, weight of the payload, and length of the trailing antenna."*

(7) *"The duration of flight."*

(8) *"The forecast time and location of impact with the surface of the earth."*

(b) *"For solar or cosmic disturbance investigations involving a critical time element, the information in paragraph (a) of this section shall be given within 30 minutes to 24 hours before beginning the operation."*

(c) *"Cancellation notice: If the operation is canceled, the person who intended to conduct the operation shall immediately notify the nearest FAA ATC facility."*

(d) *"Launch notice: Each person operating an unmanned free balloon shall notify the nearest FAA or military ATC facility of the launch time immediately after the balloon is launched."*

§101.39 Balloon position reports.

(a) *"Each person operating an unmanned free balloon shall:"*

(1) *"Unless ATC requires otherwise, monitor the course of the balloon and record its position at least every two hours; and"*

(2) *"Forward any balloon position reports requested by ATC."*

(b) *"One hour before beginning descent, each person operating an unmanned free balloon shall forward to the nearest FAA ATC facility the following information regarding the balloon:"*

- **(1)** *"The current geographical position."*
- **(2)** *"The altitude."*
- **(3)** *"The forecast time of penetration of 60,000 feet standard pressure altitude (if applicable)."*
- **(4)** *"The forecast trajectory for the balance of the flight."*
- **(5)** *"The forecast time and location of impact with the surface of the earth."*

(c) *"If a balloon position report is not recorded for any two-hour period of flight, the person operating an unmanned free balloon shall immediately notify the nearest FAA ATC facility. The notice shall include the last recorded position and any revision of the forecast trajectory. The nearest FAA ATC facility shall be notified immediately when tracking of the balloon is re-established."*

(d) *"Each person operating an unmanned free balloon shall notify the nearest FAA ATC facility when the operation is ended."*

FCC (Title 47: Telecommunication, Chapter I, Subchapter B, Part 22 [46])

§22.925 Prohibition on airborne operation of cellular telephones

"Cellular telephones installed in or carried aboard airplanes, balloons or any other type of aircraft must not be operated while such aircraft are airborne (not touching the ground). When any aircraft leaves the ground, all cellular telephones on board that aircraft must be turned off."

Moreover, as the sovereignty of the airspace relies on the countries itself, they have the right to establish certain areas where the flight can be restricted, forbidden either permanent or temporally or not recommended. In the case of Spain, the Spanish AIP (see **Figure 29**) established the following areas [47]:

- Delta Area, also known as Danger area. Is an airspace of defined dimensions within which activities dangerous to the flight of aircraft may exist at specified times.
- Papa Areas, also known as Prohibited areas. Is an airspace of defined dimensions, above the land areas or territorial water of a State, within which the flight of aircraft is prohibited.
- Romeo Areas, also known as Restricted areas. Is an airspace of defined dimensions, above the land areas or territorial waters of a State, within which the flight of aircraft is restricted in accordance with certain specified conditions.

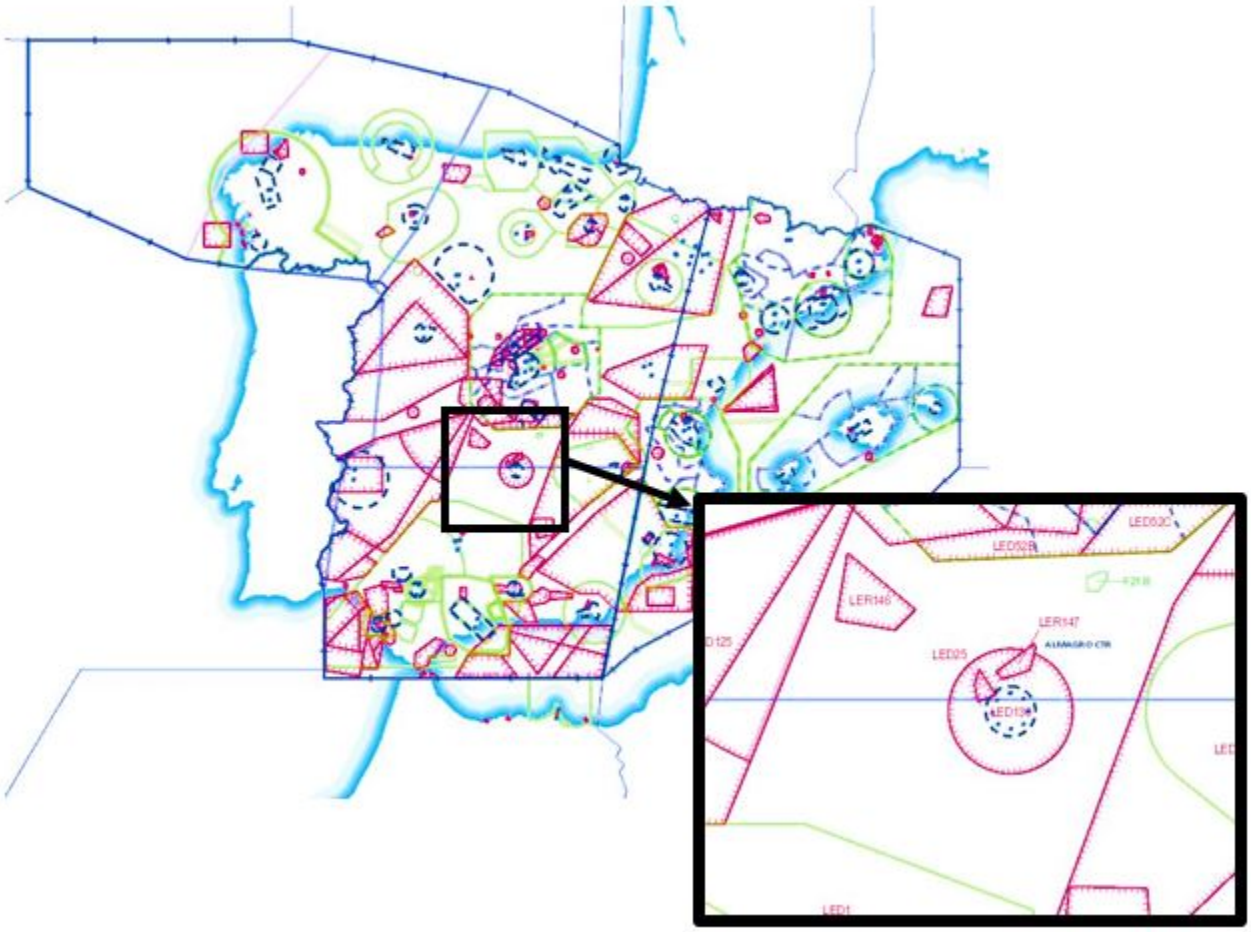

Figure 29: Spanish AIP map with a zoom in the launch area of this project [48]

4.2 Socio-economic Framework

Currently, several governmental agencies such as NASA (National Aeronautics and Space Administration) promoted effective drivers of investments in the global space economy, encoring traditional as well as non-traditional companies, to look beyond satellites for new opportunities in the commercial space markets [49].

"The results of these studies provide insights into the potential economic impacts of new space-based capabilities and applications which in turn helps guide our investments in technology development", said Steve Jurczyk, associate administrator for the Space Technology Mission Directorate at NASA.

In 2017, the space sector increased up to 4% of the global economy. The majority of this growth was through the commercial economic expansion of products, services, and infrastructures. However, the entrepreneurship also plays an important role by contributing with their technical innovations, cost efficiencies, and new business models [50].

Moreover, some enterprising companies have initiated the commercial space tourism industry by seeking the opportunity of developing ways for customers to experience stratospheric flights. Some companies such as the company Zero2Infinity, are planning to use high altitude balloons, while others endeavor to employ powered space vehicles. In recent years, several prototypes have been built and tested out, although to date no commercial flights have been made [50].

4.3 Project budget

This project develops the design of a flight trajectory simulator, where the flight predictions allow the user to obtain an approximate image of the landing zone as well as ensure that the margin of uncertainty is outside of and away of any of the restricted areas mention at the end of **Section 4.1**. Hence, a verification flight will be launched in order to ensure that the results of the simulation are correct.

The resources needed for the development of the project are:

1. **Labor force**
    - 1 Junior Aerospace Engineer (student)
    - 1 Aerospace Engineering Teacher (only as a supervisor)
2. **Software resources**
    - MATLAB
    - Windows
    - Google Earth
    - Microsoft Office
3. **Other resources**
    - Internet connexion for 8 months
    - Hard drive (Back-up)

Therefore, as the budget is one of the key factors in the development of a project, a rough estimation of the direct and indirect cost associated with it will be performed.

Direct costs

Direct costs are traceable expenses that can be easily attributed to a project. In this case, the direct costs can be classified as:

- Labor force The labor force has been calculated taking into account the hours needed by the junior aerospace engineer to develop the corresponding simulator, as well as the hours invested by the supervisor to verify that the results were meaningful. For it, the labor cost of the student has been stipulated considering a cost of 6 €/*hour*, taking as a reference the averaged salary of an undergraduate internship (850 − 900 €). On the other hand, the labor cost of the teacher has been calculated taking the averaged cost of 30 €/*hour* as a rough estimation obtained from the tables of cost for a Ph.D. professor of the "University Carlos III of Madrid" [51].

  As it can be observed in **Table 3**, the following labor cost is broken down:

Group	No. of workers	Price per hour	No. of hours	Price per worker
Student	1	6 €/hour	670	4020 €
Teacher (Supervisor)	1	30 €/hour	100	3000 €
			Total cost (Labor force)	7020 €

Table 3: Labor force cost

- Software resources The software licenses needed for the development, implementation, and verification of this project can be classified as (see **Table 4**):

Software	Version	License	Price
MATLAB	2018b	Academic student	86 €
Windows	10	Home	139 €
Google Earth	Pro 7.3.2	Home	Free
Microsoft Office	2016	Home	120 €
		Total cost	345 €

Table 4: Software resources cost

Indirect costs

Indirect costs are those necessary to keep your project in operation such as Internet connexion. These resources are needed in order to ensure that the advances of the project remain safe and that the progress can continue to move forward (see **Table 5**).

However, the depreciation of the computer and the hard-drive are also considered indirect costs. Therefore, a life cycle of 4 years and a linear depreciation over the whole lifetime will be assumed. Then, the amortization cost of the following resources can be computed as follows:

$$Amortization = Price \cdot \frac{Depreciation}{Lifetime} \tag{45}$$

1. Computer:

$$Amortization = 515\,€ \cdot \frac{8 \text{ months}}{4\text{year} \cdot 12\frac{months}{year}} \approx 85.8\,€$$

2. Hard-drive:

$$Amortization = 90\,€ \cdot \frac{8 \text{ months}}{4\text{year} \cdot 12\frac{months}{year}} \approx 15\,€$$

Moreover, a percentage of 10% will be established in order to considered the rest of the indirect costs of the project that are not that easy to calculate.

Concept	No. of units	Price	Time used	Depreciation time	Imputable cost
Computer	1	515 €	8 months	48 months	85.8 €
Hard-drive (Back-up)	1	85 €	8 months	48 months	15 €
Internet connexion	1	30 €/month	8 months	N/A	240 €
Others depreciations	N/A	152 €	N/A	N/A	15.2 €
				Total cost	356 €

Table 5: Indirect resources cost

Finally, the cost of the project can be observed in **Table 6**.

Concept	Price
Labor force	7020 €
Software resources	345 €
Other resources	356 €
Total cost	7721 €

Table 6: Final project budget

4.4 Project Planning

It is well known that the success of a project is given by diverse factors. However, having a well-organized project is one of the key factors to consider.

Therefore, a prior planning of the development of this project has been created taking into account the time needed to perform each of the tasks, as well as the maximum time of 8 months to successfully fulfill all the established goals. As it can be observed in the table below (see **Table 7**), the following activities were considered.

Task	Duration
Approach and description of the problem	5 days
Investigation of the topic	18 days
Material selection	12 days
Goal planning	10 days
Development of the models	24 days
Wind data research	10 days
Implementation of the code	60 days
Comparison with other simulators	25 days
Verification and validation of the simulator	7 days
Analysis of the results	10 days
Thesis writing	42 days
Presentation preparation	12 days
Total number of days needed	235 days

Table 7: Summary of the tasks and time needed for each of them

Taking into consideration the days needed to develop each of the tasks, a Gantt chart (see **Figure 30**) has been created. It is important to highlight that:

- The green color indicates the phases prior to the development of the project.
- The blue color indicates the phases of implementation of the trajectory simulator.
- The red color indicates the phases of documentation of the project.

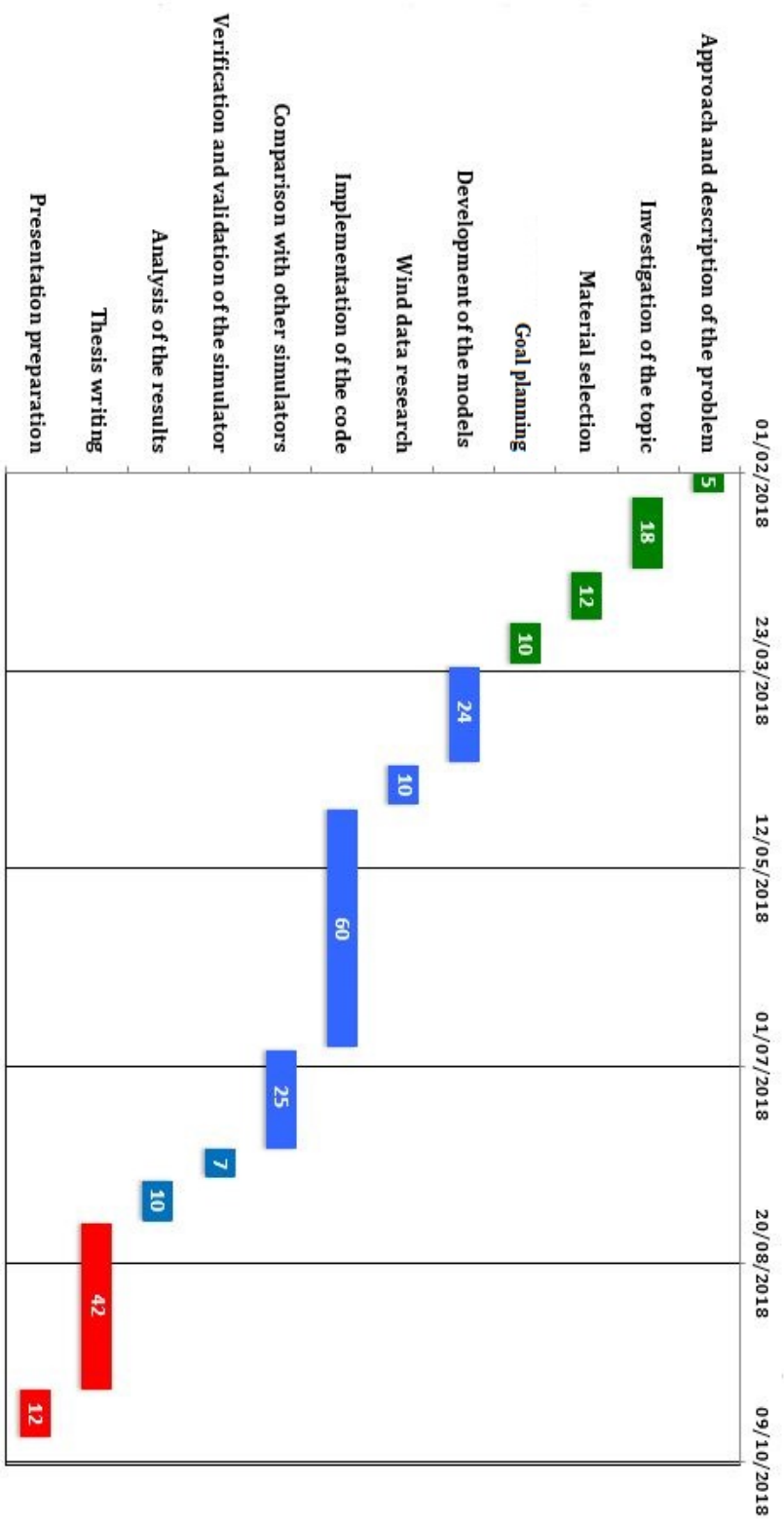

Figure 30: Gantt chart of the project

5 Contest: "TFG Emprende"

5.1 The contest

The "TFG Emprende" contest aims to be an instrument for students of the University Carlos III of Madrid to get involved in the culture of entrepreneurship, innovation, and adoption of the development of new technologies [52]. Thus, the 50 students selected to participate in the 5^{th} call of this contest will have to develop an idea of innovation based on their current thesis project.

Figure 31: TFG Emprende Contest logo

In addition, several workshops given by professionals in different sectors took place, in which two main blocks were exposed. These blocks are:

- **Block I: Innovation and competitive advantage**

  Focused on giving an overview of what does the innovation concept means and introducing the different types of entrepreneurship to obtain a clear idea and be able to apply it to the innovation project.

- **Block II: Business Canvas model**

  Focused on giving a clear understanding of the difference between a business plan and a business model, as well as introducing an outstanding business model known as the Canvas business model.

5.2 The Entrepreneur project

After several weeks searching for information regarding high-altitude balloons, as well as thinking about the idea of bringing this technology in an efficient way to those who need it most, the thought of taking part in the contest was becoming important.

As Kevin Kruse said, *"Life is about making an impact, not making an income."*

Therefore, the idea of innovation chosen for the contest will be focused on a social project. Hence, a depth understanding of the main advantages of the developed software during this study, as well as exploiting the idea of expanding Internet connectivity with stratospheric balloons proposed by Google (Loon project), will consolidate the basic pillars of this innovation project idea.

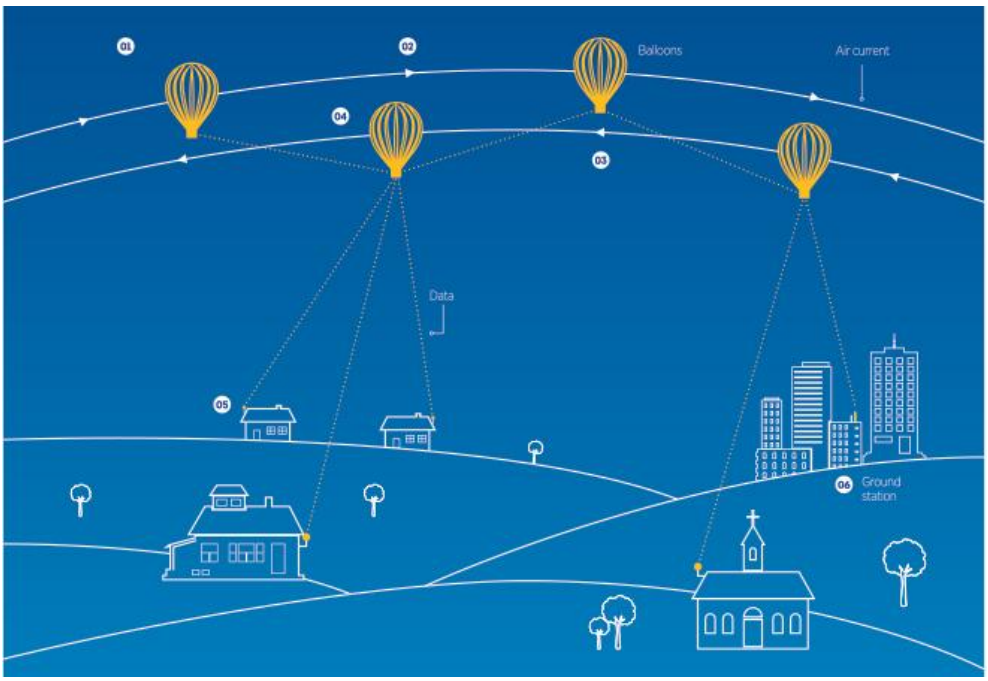

Figure 32: Loon project sponsored by Google [53]

During the first phases of the project, the idea was consolidated through several tools focused on innovative development such as the PESTEL (Political-Economic-Social-Technological-Environmental-Legal) analysis. The aim of this phase was to orientate the project towards a solution to an existing problem or need.

In the second phase, an innovative Canvas model (see **Figure 33**) was performed in order to consolidate the idea.

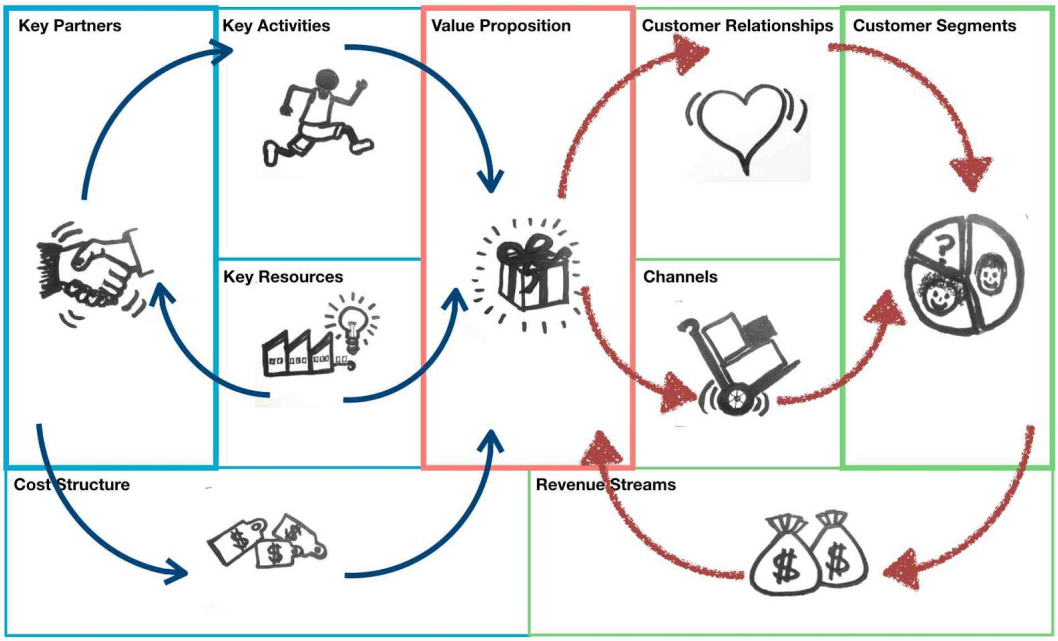

Figure 33: Innovative Canvas model structure [54]

As it can be observed in **Figure 33**, the elements of the business Canvas model can be identified answering the following questions [54]:

1. **Key Partner:** What can the company outsource to partners so it can focus on its key activities?
2. **Key Activities:** What key activities company does to deliver the value proposition?
3. **Key Resources:** What unique assets company has in order to compete?
4. **Value Proposition:** Why would customers want to buy and use the product? Why is it different than other similar products?
5. **Customer Relationships:** How do you interact with your customers through their "journey" with the product?
6. **Channels:** How do you promote, sell and deliver your products to customers?
7. **Customer Segments:** Who are your customers? What do they feel, see, think?
8. **Cost Structure:** What are the business' major cost drivers? How are they linked to revenue?
9. **Revenue Streams:** How does the business earn revenue from the value propositions?

Furthermore, a poll was conducted to analyze the social impact that the project would have. After evaluating the answers and observing a positive impact in the society, the idea was finally established.

Concluding, the idea of the project will be presented as: "Precise trajectory simulator of high-altitude balloons developed to help to deliver Internet connectivity, through stratospheric balloons, to hospitals and NGOs missions in developing countries. Aiming to provide a faster communication between them as well as improving the quality of their service, with the final purpose of saving as many lives as possible."

In order to ensure an accurate flight path predicted by the simulator, some additional tests need to be performed such as evaluating the maximum payload that the balloon can lift or a depth study of the maximum coverage area that these antennas can provide at that altitudes. However, these tests are beyond the scope of this thesis.

Although, under the slogan *"They say that the road is steep, but also that the views are beautiful. Don't you think it's worth trying?"*, we will keep working on it until the unimaginable becomes reality.

Figure 34: Innovative idea, working towards it [55]

6 Conclusions and further considerations

6.1 Conclusion

The main objective of this project was the development and implementation of a software able to predict the trajectory of a high-altitude balloon. Therefore, all the relevant physical properties of a rubber balloon were carefully modeled and implemented in a MATLAB code, extracting the wind data from the NOAA source to create an accurate trajectory simulation program.

For it, an in-depth study of the ISA atmospheric model and the main parameters that influence the inflation of a rubber-like balloon was conducted.

Afterward, the Mooney-Rivlin model and the Gent-Gent model, as well as the non-linear model, were developed in order to investigate the importance of the elastic effects of the rubber of the balloon on the prediction of the trajectory. The results of each of the models regarding the radius evolution, the lifted mass, the ascent velocity, and the membrane pressure were compared, concluding that in this specific case the elastic effects do not need to be considered, as the membrane pressure obtained at any of the altitudes of the flight is much smaller than the ambient pressure, and hence, it can be neglected.

Then, the kinetic equations of motion of the HAB were solved taking into account that the horizontal motion is mainly influenced by the wind speed, whereas the vertical motion is limited by the elastic limit of the rubber.

Finally, a validation of the software was performed by comparing its predicted trajectory with the one obtained from HABHUB and ASTRA. This comparison proved that the developed software is pretty accurate, as the trajectory obtained follows almost the same flight path that the one predicted by the other two web-based predictors. Moreover, a similar burst location, as well as burst altitude, is obtained in each of the three predictors.

6.2 Further considerations

As it was mentioned before, a final validation of the software will be performed after the data from the launch of the balloon, intended for October-November 2018, is recollected.

Furthermore, some improvements can be considered such as implementing the thermal effects of the balloon, choose a more precise atmospheric model, i.e. one closer to the launch point such as the AEMET in this case, or developed the prediction of the trajectory for the descent phase.

Hopefully, these steps towards the exact prediction of the trajectory of the high-altitude balloons will drive to promote the used of these type of devices for space missions, social purposes such as the one exposed in this thesis for "TFG Emprende" or educational purpose.

References

[1] M. Safonova, K. Nirmal, A. G. Sreejith, M. Satpodar, A. Suresh, A. Prakash, J. Mathew, J. Murthy, D. Anand, B. V. N. Kapardhi, B. Suneel Kumar & P. M. Kulkarni, *Measurements of Gondola Motion on a Stratospheric Balloon Flight*, Indian Institute of Astrophysics, Bangalore & Tata Institute of Fundamental Research, Balloon Facility, Hyderabad.

[2] *"History of Ballooning - Space Kit"*, Sites.google.com, 2017. [Online]. Available: https://sites.google.com/a/mtlsd.net/citizen-science/resources/history-of-ballooning.

[3] *"The History of Hot Air Ballooning"*, Altitudeballoons.co.uk, 2018. [Online]. Available: https://www.altitudeballoons.co.uk/Brief-History.html.

[4] *"A Short History of Ballooning — NOVA — PBS"*, Pbs.org, 2018. [Online]. Available: http://www.pbs.org/wgbh/nova/space/short-history-of-ballooning.html.

[5] *"The First Gas Balloon Flight - British Balloon Museum & Library"*, British Balloon Museum & Library, 2018. [Online]. Available: http://www.bbml.org.uk/2017/08/first-gas-balloon-flight/.

[6] *"High-Altitude Ballooning History — World View Enterprises"*, Worldview.space, 2018. [Online]. Available: https://worldview.space/history/.

[7] D.L. Jimenéz Higueras, *Design of different elements of a pressurized capsule for stratospheric balloons*, Universitat Politècnica de Catalunya, Escola Tècnica Superior d'Enginyeries Industrial i Aeronàutica de Terrassa, June 2014.

[8] L.Grush, *Inside World View, the company that wants to take you into the stratosphere with a balloon*, The Verge, February 24th, 2017. [Online]. Available: https://www.theverge.com/2017/2/24/14708614/world-view-new-hq-stratosphere-balloon-space-tourism.

[9] V. Jewtoukoff, R. Plougonven, A. Hertzog, C. Snyder & G. Romine, *On the Prediction of Stratospheric Balloon Trajectories: Improving Winds with Mesoscale Simulations*, Journal of Atmospheric and Oceanic Technology , Boston Tomo 33, N.º 8, August 2016.

[10] D. Gerson, *"Balloon Overview"*, Global Space Balloon Challenge, December 2015. [Online]. Available: http://community.balloonchallenge.org/t/balloon-overview/665.

[11] *"NASA's Super Pressure Balloon to Launch from Wanaka Airport"*,N. Airport, Nzairports.co.nz. [Online]. Available: https://www.nzairports.co.nz/resource-library/nasas-super-pressure-balloon-to-launch-from-wanaka-airport/.

[12] *HABHUB*. [Online]. Available: http://habhub.org/

[13] L.W. Renegar, *A Survey of Current Balloon Trajectory Prediction Technology*, University of Maryland, College Park, MD, 20742. [Online]. Available: https://via.library.depaul.edu/cgi/viewcontent.cgi?referer=&httpsredir=1&article=1125 &context=ahac.

[14] *ASTRA High Altitude Balloon Flight Planner*. [Online]. Available: http://astra-planner.soton.ac.uk/

[15] Talay,T.A., *Introduction to the Aerodynamics of Flight*, NASA SP-367, National Aeronautics and Space Administration, Washington D.C.,1975,p.6-9.

[16] J. Hilario, *Chapter 1: Generalities and Operating Environment*, Bioengineering and Aerospace Engineering Department, Universidad Carlos III de Madrid, 2017.

[17] B. Dunbar, *Earth's Atmospheric Layers*, NASA/Goddard, National Aeronautics and Space Administration, January 22th 2013. [Online] Available: http://www.nasa.gov/mission-pages/sunearth/science/atmosphere-layers2.html.

[18] *"Layers of Earth's Atmosphere | UCAR Center for Science Education"*, Scied.ucar.edu, 2018. [Online]. Available: https://scied.ucar.edu/atmosphere-layers.

[19] *"Layers of the atmosphere"*, NIWA, 2018. [Online]. Available: https://www.niwa.co.nz/education-and-training/schools/students/layers.

[20] C. Ferguson, *Basic Properties of the Atmosphere*, 2015. [Online]. Available: https://slideplayer.com/slide/6901967/

[21] Airbus, *Getting to Grips with Aircraft Performance*, Airbus Industrie, Customer Services, Blagnac, 2000, p.11-16.

[22] *"Archimedes' principle"*. Encyclopædia Britannica. Encyclopædia Britannica Online. Encyclopædia Britannica Inc., 2018. Web. 06 sep. 2018 [Online]. Available: https://www.britannica.com/science/Archimedes-principle.

[23] C. Hodanbosi,*Buoyancy: Archimedes principle*, Jun. 2014. [Online]. Available: https://www.grc.nasa.gov/www/k12/WindTunnel/Activities/buoy-Archimedes.html.

[24] "Physics Mass and Weight", www.tutorialspoint.com, 2018. [Online]. Available: $https://www.tutorialspoint.com/physics_part1/physics_mass_and_weight.htm$.

[25] N. Yajima, N. Izutsu, T. Imamura, and T. Abe, Scientic Ballooning : *Technology and Applications of Exploration Balloons Floating in the Stratosphere and the Atmospheres of Other Planets*. Springer-Verlag New York, 2009.

[26] A.L. Morris, *Scientific Ballooning Handbook*, NCAR (National Center for Atmospheric Research) technical note, Boulder, Colorado, May 1975, vol. TN, 1A-99.

[27] G. R. Conrad and E. J. Robbins, *Determination of Balloon Drag. AIAA International Balloon Technology Conference*, 1991, vol. Paper 1991-3666.

[28] K. Timberlake, *MasteringChemistryPlus for Chemistry*. Boston, Prentice Hall, 2014.

[29] Scientific Ballooning Assessment Group, *Stratospheric Balloons: Science at the edge of the Space*, NASA (National Aeronautics and Space Administration), January 2010.

[30] F. Wheeler and R. Goodall *An Experiment On Elasticity Using Balloons*, University of Sheffield, SAS newsletter, Summer 2011.

[31] J. Gotro, *Polymers in Electronic Packaging: What Types of Polymers are Used?*,Polymer Innovation Blog, January 15,2018. [Online]. Available: https://polymerinnovationblog.com/polymers-electronic-packaging-types-polymers-used/

[32] W.A. Osborne, *The elasticity of rubber balloons and hollow viscera,* Proceedings of the Royal Society of London, Series B, 81 (1909), pg. 485–499.

[33] M. Chapman, *Weather balloon physics*, February 27,2012. [Online]. Available:http://zmatt.net/weather-balloon-physics.

[34] L. A. Mihai & A. Goriely (2017), *How to characterize a nonlinear elastic material? A review on nonlinear constitutive parameters in isotropic finite elasticity*, Proceedings, Mathematical, Physical, and Engineering Sciences. [Online]. Available: http://doi.org/10.1098/rspa.2017.0607

[35] L. M. Kanner, *Inflation of strain-stiffening rubber-like thin spherical shells*, Department of Civil Engineering, University of Virginia. [Online]. Available: https://pdfs.semanticscholar.org/78b7/ec446dd9c5edb527c9b30f8e11e5d5439b2a.pdf.

[36] A. N. Jadhav, Dr. S. R. Bahulikar & N. H. Sapate, *Comparative Study of Variation of MooneyRivlin Hyperelastic Material Models under Uniaxial Tensile Loading*, Maharashira, India, Vol. 2, April 2016. [Online]. Available: *http* : $//www.ijariie.com/AdminUploadPdf/Comparative_Study_of_Variation_of_Mooney_Rivlin_Hyperelastic_Material_Models_under_Uniaxial_Tensile_Loading_ijariie2865.pdf$

[37] A.N. Gent, *A new constitutive relation for rubber*, Rubber Chem. Technol., vol.69, 1996, pg. 59–61.

[38] E. Pucci, G. Saccomandi, *A note on the Gent model for rubber-like materials*, Rubber Chemistry and Technology, vol. 75, 2002, pg. 839–851.

[39] *"About Our Agency — National Oceanic and Atmospheric Administration"*, Noaa.gov, 2018. [Online]. Available: http://www.noaa.gov/about-our-agency.

[40] *"What is the significance of the NOAA logo?"*, Oceanservice.noaa.gov, 2018. [Online]. Available: https://oceanservice.noaa.gov/facts/noaalogo.html.

[41] *The NOMADS Project — National Centers for Environmental Information (NCEI) formerly known as National Climatic Data Center (NCDC)*, Ncdc.noaa.gov, 2018. [Online]. Available: https://www.ncdc.noaa.gov/nomads.

[42] *File: ECEF ENU Longitude Latitude Upwardness relationships*, Wikimedia Commons, 2018. [Online]. Available: https://commons.wikimedia.org/wiki/File:ECEF-ENU-Longitude-Latitude-Upwardness-relationships.svg.

[43] *"Weather Balloon Safety & Regulations — OLHZN High Altitude Balloons"*, OLHZN High Altitude Balloons — Canandaigua, NY, 2018. [Online]. Available: https://www.overlookhorizon.com/flight-safety/.

[44] European Aviation Safety Agency (EASA), *Balloon Rule Book*, EASA eRules: aviation rules for the 21st century, March 2018. [Online]. Available: https://www.easa.europa.eu/sites/default/files/dfu/Balloon

[45] Federal Aviation Agency (FAA), *Title 14: Aeronautics and Space*, Electronic Code of Federal Regulation, September 12th, 2018. [Online]. Available: https://www.ecfr.gov/cgi-bin/text-idx rgn=div8&node=47:2.0.1.1.2.8.27.12.

[46] Federal Communications Commission (FCC), *Title 47: Telecommunication*, Electronic Code of Federal Regulation, September 12th, 2018. [Online]. Available: https://www.ecfr.gov/cgi-bin/text-idxrgn=div5&node=14:2.0.1.3.15#sp14.2.101.d.

[47] J. Lloret, *Introduction to Air Navigation: A technical and operational approach*, Createspace, 2015, vol. Chapter 7.

[48] NOTAMs en INSIGNIA, ENAIRE, December 21st, 2017. [Online]. Available: https://ais.enaire.es/insignia/navegador/

[49] *"NASA Selects Economic Research Studies to Examine Investments in Space"*, NASA, September 13th, 2017. [Online]. Available:

https://www.nasa.gov/directorates/spacetech/emergingspace/feature/NASA-Selects-Economic-Research-Studies.

[50] J. Chan-Hao,*Entrepreneurship and its Role in Space Industry*, Working Group, Industry & Wang, DOC: 10.13140/RG.2.1.3178.0242. , September 2014.

[51] *"Retribuciones UC3M", Universidad Carlos III de Madrid, 2016.* [Online]. Available: https://www.uc3m.es/ss/Satellite/UC3MInstitucional/es/TextoMixta/1371208973960.

[52] *"Trabajo Fin de Grado Emprende — UC3M"*, Uc3m, 2017. [Online]. Available: https://www.uc3m.es/ss/Satellite/UC3MInstitucional/es/TextoDosColumnas/1371244096036/Trabajo-Fin-de-Grado-Emprende.

[53] N.G. News Desk, *Google Project Loon to solve Indian rural internet issues*, November 3rd, 2015. [Online]. Available: https://www.newsgram.com/google-project-loon-to-solve-indian-rural-internet-issues

[54] V. Knezevic, *"4 Brilliant Benefits of the Business Model Canvas"*, AWW. [Online]. Available: http://blog.awwapp.com/business-model-business-model-canvas/.

[55] Instituto del Sur, *"Importancia de la innovación en el sector turístico - Entorno Turístico"*, Entorno Turístico. [Online]. Available: https://www.entornoturistico.com/innovacion-sector-turistico/.

Appendix A

Technical Specification for Meteorological Balloon

As it can be obtained from the Indian company *"PAWAN Exports"* (see their website for more details) , the specifications for the PAWAN rubber balloon are the following:

SPECIFICATION	CPR-1600
Mass [g]	1600
Payload [g]	1100
Recommend free lift [g]	1310
Nozzle lift [g]	2310
Gross lift [g]	3910
Diameter at release [m]	1.94
Rate of ascent [m/min]	325
Diameter at burst [meters]	9.5
Bursting altitude [m]	34000
Neck diameter [m]	0.085
Neck length [m]	0.20-0.22
Color	Uncolored / White

Table 8: Technical specifications for the PAWAN-1600gm

Note: The manufacturer said that *"small or large neck diameter does not affect the balloon performance. Moreover, the diameter at release is for recommended free lift and above mentioned payload. Hence, if the free lift or payload weight change, the diameter at release will consequently change."*

Appendix B

MATLAB code

In this section, the MATLAB code implemented for the development of the software predictor, as well as all the results explained in this thesis, can be obtained in the following link: High-altitude Trajectory Predictor

In this folder, the following files are found:

- **DV folder**: In this folder, the wind data downloaded from the NOAA source is founded. This folder contains data from June to September 2018.

- **Nctoolbox folder:** In this folder, the *"setup nctoolbox"* script is obtained. This script needs to be run before running the main script, in order to implement this extra toolbox in MATLAB.

- **Equations of motion:** This file is the main script of the predictor, where all the specifications of the balloon are implemented. Moreover, all the plots explained in this thesis are obtained after running this script. The inputs need are the altitude of the launch point, as well as the longitude and latitude of the this location.

- **Elasticity function:** In this file, the non-linear model, as well as the Mooney-Rivlin model and the Gent-Gent model, have been implemented in order to evaluate the elastic effects of the rubber of the balloon in the flight-path.

- **MyISA function:** In this file, the International Standard Atmosphere (ISA) model has been implemented for the different layer of the Atmosphere.

- **Interpolate nomads:** In this file, the interpolation of the wind data obtained from the NOAA source is performed.

- **OdeinX function:** In this file, the Ordinary Differential Equation in the x-direction is solved.

- **OdeinY function:** In this file, the Ordinary Differential Equation in the y-direction is solved.

- **OdeinZ function:** In this file, the Ordinary Differential Equation in the z-direction is solved.

Appendix C

Abbreviation

- **AEMET** = Agencia Estatal de Meteorología
- **ASTRA** = Atmospheric Science Through Robotic Aircraft
- **CUSF** = Cambridge University Space Flight
- **EASA** = European Aviation Safety Agency
- **EU** = European Union
- **FAA** = Federal Aviation Administration
- **FCC** = Federal Communication Commission
- **GFS** = Global Forecasting System
- **GG** = Gent-Gent
- **HAB** = High-altitude balloons
- **ICAO** = International Civil Aviation Organization
- **ISA** = International Standard Atmosphere
- **MSL** = Mean Sea Level
- **NASA** = The National Aeronautics and Space Administration
- **NGOs** = Non-Governmental Organizations
- **NOAA** = National Oceanic and Atmospheric Administration
- **NOMADS** = National Operational Model Archive and Distribution System
- **NWP** = Numerical Weather Prediction
- **PESTEL** = Political-Economic-Social-Technological-Environmental-Legal analysis
- **SEF** = Strain Energy Function
- **UKHAS** = UK High Altitude Society
- **UV** = Ultraviolet